RESEARCH ARTICLE

Site-specific effects of neurosteroids on $GABA_A$ receptor activation and desensitization

Yusuke Sugasawa[1], Wayland WL Cheng[1], John R Bracamontes[1], Zi-Wei Chen[1,2], Lei Wang[1], Allison L Germann[1], Spencer R Pierce[1], Thomas C Senneff[1], Kathiresan Krishnan[3], David E Reichert[2,4], Douglas F Covey[1,2,3,5], Gustav Akk[1,2], Alex S Evers[1,2,3]*

[1]Department of Anesthesiology, Washington University in St. Louis, St. Louis, United States; [2]Taylor Family Institute for Innovative Psychiatric Research, Washington University in St. Louis, St. Louis, United States; [3]Department of Developmental Biology, Washington University in St. Louis, St. Louis, United States; [4]Department of Radiology, Washington University in St. Louis, St. Louis, United States; [5]Department of Psychiatry, Washington University in St. Louis, St. Louis, United States

Abstract This study examines how site-specific binding to three identified neurosteroid-binding sites in the $\alpha_1\beta_3$ $GABA_A$ receptor ($GABA_AR$) contributes to neurosteroid allosteric modulation. We found that the potentiating neurosteroid, allopregnanolone, but not its inhibitory 3β-epimer epi-allopregnanolone, binds to the canonical β_3(+)–α_1(-) intersubunit site that mediates receptor activation by neurosteroids. In contrast, both allopregnanolone and epi-allopregnanolone bind to intrasubunit sites in the β_3 subunit, promoting receptor desensitization and the α_1 subunit promoting effects that vary between neurosteroids. Two neurosteroid analogues with diazirine moieties replacing the 3-hydroxyl (KK148 and KK150) bind to all three sites, but do not potentiate $GABA_AR$ currents. KK148 is a desensitizing agent, whereas KK150 is devoid of allosteric activity. These compounds provide potential chemical scaffolds for neurosteroid antagonists. Collectively, these data show that differential occupancy and efficacy at three discrete neurosteroid-binding sites determine whether a neurosteroid has potentiating, inhibitory, or competitive antagonist activity on $GABA_ARs$.

***For correspondence:** eversa@wustl.edu

Competing interests: The authors declare that no competing interests exist.

Funding: See page 28

Received: 20 January 2020
Accepted: 20 September 2020
Published: 21 September 2020

Reviewing editor: Cynthia M Czajkowski, University of Wisconsin, Madison, United States

Introduction

Neurosteroids (NS) are endogenous modulators of brain development and function and are important mediators of mood (***Belelli and Lambert, 2005***; ***Mitchell et al., 2008***; ***Represa and Ben-Ari, 2005***; ***Grobin et al., 2006***). Exogenously administered NS analogues have been clinically used as anesthetics and anti-depressants and have therapeutic potential as anti-epileptics, neuroprotective agents and cognitive enhancers (***Belelli and Lambert, 2005***; ***Mitchell et al., 2008***; ***Akk et al., 2007***; ***Reddy and Estes, 2016***; ***Kharasch and Hollmann, 2015***; ***Gunduz-Bruce et al., 2019***; ***Zorumski et al., 2019***). The principal target of NS is the γ-aminobutyric acid type A receptor ($GABA_AR$). NS can either activate or inhibit $GABA_ARs$. Positive allosteric modulatory NS (PAM-NS) such as allopregnanolone (3α5αP) potentiate the effect of GABA on $GABA_AR$ currents at low concentrations and directly activate the receptors at higher concentrations (***Akk et al., 2007***; ***Akk et al., 2010***; ***Chen et al., 2019***; ***Olsen, 2018***). Negative allosteric modulatory NS (NAM-NS), such as epi-allopregnanolone (3β5αP) or pregnenolone sulfate (PS) inhibit $GABA_AR$ currents (***Akk et al., 2001***; ***Wang et al., 2002***; ***Shen et al., 2000***; ***Lundgren et al., 2003***; ***Seljeset et al., 2018***). In addition to

enhancing channel opening, PAM-NS increase the affinity of the $GABA_AR$ for orthosteric ligand binding, an effect thought to be mechanistically linked to channel gating (**Chen et al., 2019**; **Harrison et al., 1987a**).

$GABA_ARs$ are pentameric ligand-gated ion channels (pLGIC) composed of two α-subunits (α_{1-6}), two β-subunits (β_{1-3}) and one additional subunit (γ_{1-3}, δ, ε, θ or π) (**Sigel and Steinmann, 2012**; **Sieghart, 2015**; **Olsen and Sieghart, 2008**). Each subunit is composed of a large extracellular domain (ECD), a transmembrane domain (TMD) formed by four membrane-spanning helices (TM1-4), a long intracellular loop between TM3 and TM4, and a short extracellular C-terminus (**Akk et al., 2007**; **Sigel and Steinmann, 2012**; **Sieghart, 2015**; **Laverty et al., 2019**). NS modulate $GABA_ARs$ by binding to sites within the TMDs (**Belelli and Lambert, 2005**; **Mitchell et al., 2008**; **Akk et al., 2007**; **Reddy and Estes, 2016**; **Chen et al., 2019**; **Miller et al., 2017**; **Laverty et al., 2017**; **Hosie et al., 2006**; **Hosie et al., 2009**; **Chen et al., 2018**; **Sugasawa et al., 2019**). Specifically, the α subunit TMDs are essential to the actions of PAM-NS (**Chen et al., 2019**; **Miller et al., 2017**; **Laverty et al., 2017**; **Chen et al., 2018**; **Sugasawa et al., 2019**). Mutagenesis studies in $\alpha_1\beta_2\gamma_2$ $GABA_ARs$ have identified several residues in the α_1 subunit, notably Q242 and W246 in TM1, as critical to NS potentiation of GABA-elicited currents (**Hosie et al., 2006**; **Hosie et al., 2009**; **Akk et al., 2008**). Crystallographic studies have subsequently shown that, in homo-pentameric chimeric receptors in which the TMDs are derived from either α_1 (**Laverty et al., 2017**; **Chen et al., 2018**) or α_5 subunits (**Miller et al., 2017**), the NS 3α,21dihydroxy-5α-pregnan-20-one (3α5α-THDOC), pregnanolone and alphaxalone bind in a cleft between the α subunits, with the C3-hydroxyl substituent of the steroids interacting directly with Q242 in the α subunit (αQ242). PAM-NS activate these chimeric receptors, and their action is blocked by αQ242L and αQ242W mutations. These studies posit a single canonical intersubunit binding site for NS action that is conserved across the six α subunit isoforms (**Miller et al., 2017**; **Laverty et al., 2017**; **Chen et al., 2018**).

An alternative body of evidence suggests that PAM-NS modulation of $GABA_AR$ function is mediated by multiple mechanisms and/or binding sites. Site-directed mutagenesis has identified multiple disparate residues on $GABA_ARs$ that affect NS-induced activation, suggestive of two NS-binding sites: one site mediating potentiation of GABA responses and the other mediating direct activation (**Hosie et al., 2006**; **Hosie et al., 2009**). Single channel electrophysiological studies (**Akk et al., 2007**; **Akk et al., 2010**; **Akk et al., 2004**) as well as studies examining neurosteroid modulation of [^{35}S]t-butylbicyclophosphorothionate (TBPS) binding (**Evers et al., 2010**), have also identified multiple distinct effects of NS, with various structural analogues producing some or all of these effects, consistent with multiple NS-binding sites (**Hosie et al., 2006**; **Hosie et al., 2009**). Our recent photolabeling studies have confirmed that there are multiple PAM-NS-binding sites on $\alpha_1\beta_3$ $GABA_ARs$ (**Chen et al., 2019**). In addition to the canonical site at the interface between the TMDs of adjacent subunits (intersubunit site) (**Chen et al., 2019**; **Miller et al., 2017**; **Laverty et al., 2017**; **Chen et al., 2018**), we identified NS-binding sites within the α-helical bundles of both the α_1 and β_3 subunits (intrasubunit sites) of $\alpha_1\beta_3$ $GABA_ARs$ (**Chen et al., 2019**). 3α5αP binds to all three sites (**Chen et al., 2019**); mutagenesis of these sites suggests that the intersubunit and α_1 intrasubunit sites, but not the β_3 intrasubunit site, contribute to 3α5αP PAM activity (**Chen et al., 2019**). A functional effect for NS binding to the β_3 intrasubunit site has not been identified.

The 3α-hydroxyl (3α-OH) group is critical to NS activation of $GABA_ARs$ and 3β-OH NS lack PAM activity (**Akk et al., 2007**; **Wang et al., 2002**). Indeed, many 3β-OH NS are $GABA_AR$ NAMs (**Wang et al., 2002**; **Lundgren et al., 2003**). While molecular docking studies have suggested that the 3β-OH NS epi-pregnanolone (3β5βP) should compete for binding with PAM-NS (**Miller et al., 2017**), 3β-OH NS are non-competitive inhibitors with respect to GABA and 3α-OH NS, indicating that they are unlikely to act at the canonical PAM-binding site (**Akk et al., 2007**; **Wang et al., 2002**). Steroids with a sulfate rather than a hydroxyl at the 3-carbon are also $GABA_AR$ NAMs thought to act at sites distinct from $GABA_AR$ PAMs (**Akk et al., 2007**; **Akk et al., 2001**; **Wang et al., 2002**; **Seljeset et al., 2018**; **Park-Chung et al., 1999**). The precise location of this site is unclear, but crystallographic studies have demonstrated a possible binding site between TM3 and TM4 on the intracellular end of the α-subunit TMD (**Seljeset et al., 2018**; **Laverty et al., 2017**). While 3β-OH NS and PS both inhibit $GABA_ARs$, they likely act via interactions with distinct sites (**Akk et al., 2007**; **Akk et al., 2001**; **Wang et al., 2002**; **Lundgren et al., 2003**; **Seljeset et al., 2018**; **Miller et al., 2017**; **Laverty et al., 2017**).

The goal of the current study was to determine the specific sites underlying the PAM and NAM actions of NS. We hypothesized that various NS analogues preferentially bind to one or more of the three NS-binding sites in the $\alpha_1\beta_3$ $GABA_AR$, stabilizing distinct conformational states (i.e. resting, open or desensitized). To achieve this goal, we used two endogenous NS, the PAM-NS 3α5αP and the NAM-NS 3β5αP and two NS analogues, KK148 and KK150, in which a diazirine replaced the function-critical 3-OH group (***Jiang et al., 2016***). We examined site-specific NS binding and effects using NS photolabeling (***Sugasawa et al., 2019***; ***Budelier et al., 2017***; ***Budelier et al., 2019***; ***Cheng et al., 2018***) and measurements of channel gating and orthosteric ligand binding. The NS lacking a 3α-OH were devoid of PAM-NS activity, but surprisingly, KK148 and 3β5αP enhanced the affinity of [^{3}H]muscimol binding. We interpret this finding as evidence that these compounds preferentially bind to and stabilize desensitized receptors, since both open and desensitized $GABA_AR$ exhibit enhanced orthosteric ligand-binding affinity (***Chang et al., 2002***).

The results show that 3α5αP binds to the canonical β(+)–α(-) intersubunit site, stabilizing the open state of the receptor, whereas the 3-diazirinyl NS (KK148 and KK150) bind to this site but do not promote channel opening, and 3β5αP does not occupy this site. These data indicate that NS binding to the intersubunit sites is largely responsible for PAM activity and that the 3α-OH is critical for NS activation. In contrast, 3α5αP, 3β5αP and the 3-diazirinyl NS all bind to both the α_1 and β_3 intrasubunit sites. Occupancy of the intrasubunit sites by 3α5αP, 3β5αP and KK148 promotes receptor desensitization. KK150 occupies all three NS-binding sites on $\alpha_1\beta_3$ $GABA_ARs$, but produces minimal functional effect suggesting a possible scaffold for a general NS antagonist. These results shed new light on the mechanisms of NS allosteric modulation of channel function, and demonstrate a novel pharmacology in which related ligands bind to different subsets of functional sites on the same protein, each in a state-dependent manner, with the actions at these sites summating to produce a net physiological effect.

Results

Distinct patterns of NS potentiation and enhancement of muscimol binding

The endogenous NS, 3α5αP is known to potentiate GABA-elicited currents (***Figure 1A***) and enhance [^{3}H]muscimol binding to $\alpha_1\beta_3$ $GABA_ARs$ (***Figure 1E***; ***Chen et al., 2019***; ***Harrison et al., 1987a***). We examined a series of NS analogues with different stereochemistries or substituents in the 3- and 17-positions: 3β5αP, KK148, and KK150 (structures shown in ***Figure 1B–D***) for their ability to potentiate GABA-elicited currents and enhance orthosteric agonist ([^{3}H]muscimol) binding. 3β5αP is the 3β-epimer of 3α5αP. KK148 and KK150 are NS analogue photolabeling reagents, which have a 3-diazirinyl moiety instead of the 3-OH, and differ from each other by the stereochemistry of the 17-ether linkage (***Jiang et al., 2016***). We observed a discrepancy between the ability of these compounds to potentiate GABA-elicited currents and their ability to enhance [^{3}H]muscimol binding in $\alpha_1\beta_3$ $GABA_ARs$. None of the NS analogues lacking a 3α-OH potentiated GABA-elicited currents (***Figure 1B–D***). However, both 3β5αP and KK148 significantly enhanced [^{3}H]muscimol binding (***Figure 1E***). KK150, in contrast, did not potentiate GABA-elicited currents and minimally enhanced [^{3}H]muscimol binding (***Figure 1D–E***). Collectively, these data show that, NS analogues with different stereochemistry or substituents at the 3- and 17-positions show distinct patterns in modulation of $\alpha_1\beta_3$ $GABA_AR$ currents and orthosteric ligand binding. We hypothesized that these patterns are a consequence of the various NS analogues stabilizing distinct conformational states of the $GABA_AR$, possibly by binding and acting at different sites. Notably, the compounds with a 3-OH (3α5αP, 3β5αP) are 10-fold more potent than those with a 3-diazirine (KK148, KK150) in enhancing [^{3}H]muscimol binding (***Figure 1E***), suggesting that the 3-OH is an important determinant of binding affinity to the site(s) mediating these effects.

State-specific actions of NS analogues

To determine why 3β5αP and KK148 enhance [^{3}H]muscimol binding but do not potentiate $\alpha_1\beta_3$ $GABA_AR$ currents, we first considered the possibility that 3β5αP- and KK148-induced enhancement of [^{3}H]muscimol binding is a selective effect on intracellular $GABA_ARs$, since the radioligand binding assay was performed on total membrane homogenates, whereas the electrophysiological assays

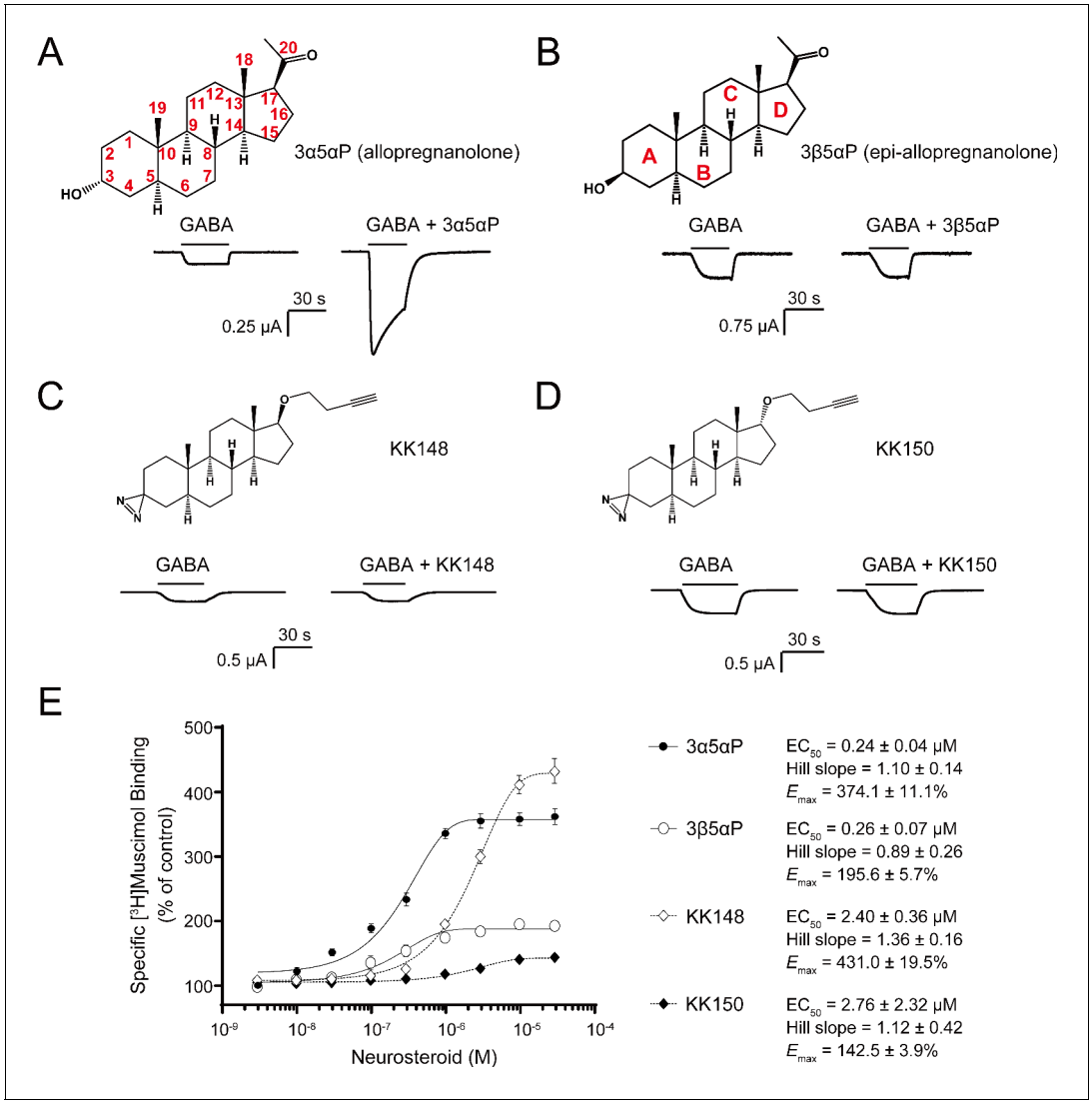

Figure 1. Distinct neurosteroid effects on potentiation of $GABA_AR$ currents and modulation of [^{3}H]muscimol binding. (**A**) Structure of allopregnanolone (3α5αP) with carbon atoms numbered and sample current traces from $\alpha_1\beta_3$ $GABA_AR$ activated by 0.3 μM GABA showing potentiation by 10 μM 3α5αP. The traces were recorded from the same cell. (**B**), (**C**) and (**D**) Structures of epi-allopregnanolone (3β5αP) with steroid rings labeled, neurosteroid analogue photolabeling reagents KK148 and KK150, respectively, and sample current traces from $\alpha_1\beta_3$ $GABA_AR$ activated by 0.3 μM GABA showing the absence of potentiation by 10 μM neurosteroids. Each pair of traces was recorded from the same cell. (**E**) Concentration-response relationship for neurosteroid modulation of [^{3}H]muscimol binding to $\alpha_1\beta_3$ $GABA_AR$. 3 nM–30 μM neurosteroids modulate [^{3}H]muscimol (3 nM) binding in a concentration-dependent manner. Data points, EC_{50}, Hill slope and maximal effect value [E_{max} (% of control): 100% means no effect] are presented as mean ± SEM (n = 6 for 3α5αP and KK148; n = 3 for 3β5αP and KK150).

The online version of this article includes the following figure supplement(s) for figure 1:

Figure supplement 1. Neurosteroid modulation of muscimol binding to intact cells.

report only from cell surface channels. NS are known to have effects on intracellular $GABA_ARs$ and have been shown to accelerate $GABA_AR$ trafficking (***Abramian et al., 2014***; ***Comenencia-Ortiz et al., 2014***; ***Smith et al., 2007***). To test this possibility, we examined [^{3}H]muscimol binding in intact cells (i.e. binding to receptors only in the plasma membrane) (***Vauquelin et al., 2015***; ***Bylund et al., 2004***; ***Bylund and Toews, 1993***) compared to permeabilized cells (plasma membranes plus intracellular membranes). Notably, [^{3}H]muscimol binding was twofold greater in permeabilized cells than in intact cells, indicating a significant population of intracellular $GABA_ARs$. KK148 enhanced [^{3}H]muscimol binding in intact cells as much or more than in permeabilized cells, indicating

that this effect is not a result of selective NS actions on intracellular receptors (***Figure 1—figure supplement 1***).

A second possibility is that 3β5αP and KK148 selectively bind to and stabilize a high-affinity non-conducting state, such as a pre-active (***Gielen and Corringer, 2018***) or a desensitized conformation of the $GABA_AR$. This is expected to result in inhibition of receptor function; however, the magnitude of the effect may be small under the experimental conditions used to generate the traces in ***Figure 1***. To examine the inhibitory effect of these NS analogues, we activated $\alpha_1\beta_3$ $GABA_AR$ with a saturating concentration (1 mM) of GABA and tested the effect of the NS on steady-state currents (***Germann et al., 2019a***). KK148 and 3β5αP both decreased steady-state currents (***Figure 2A and C***), whereas KK150 did not (***Figure 2B***). To further delineate the electrophysiological effects of these compounds, we focused on 3β5αP, since it is an endogenous NS and we had limited availability of KK148. Co-application of 3β5αP with 1 mM GABA preferentially inhibited steady-state rather than peak currents (***Figure 2—figure supplement 1***). While this result is consistent with stabilization of a desensitized state rather than a pre-active state, it is ambiguous because it is possible that the steroid has a slower onset than GABA, thus minimizing the effect on peak current. Additional evidence that 3β-NAM-NS stabilize a desensitized state includes studies examining their effects on inhibitory post-synaptic currents (***Wang et al., 2002***) and single channel currents (***Akk et al., 2001***). The evidence that NAM-NS stabilize a desensitized rather than a pre-active state is more thoroughly explored in the Discussion. In the ensuing text, we refer to the inhibition of steady-state current as desensitization.

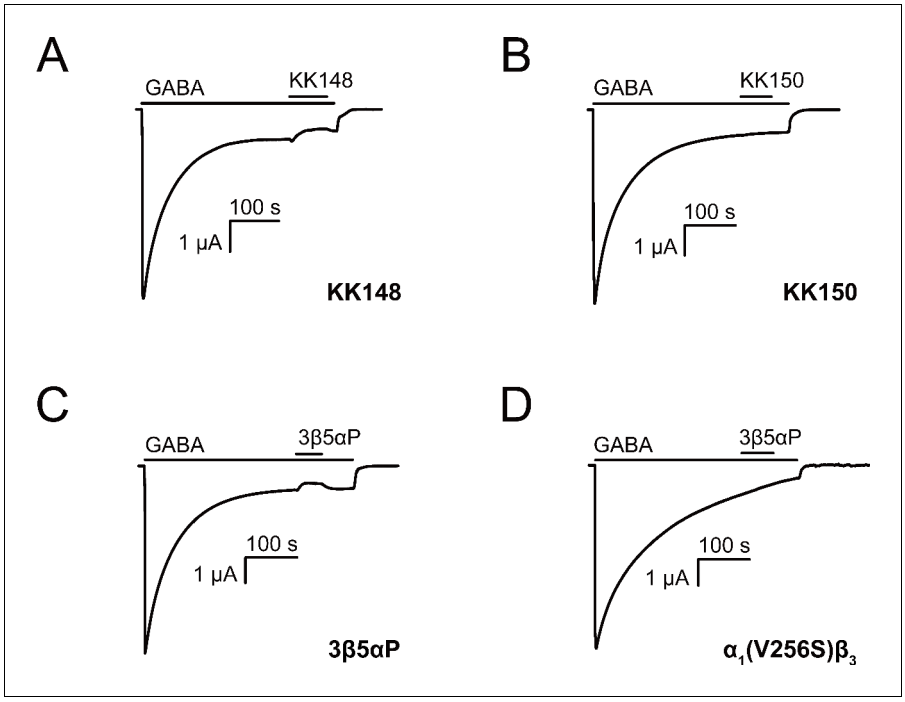

Figure 2. Neurosteroids promote steady-state desensitization of $\alpha_1\beta_3$ $GABA_ARs$. Representative traces showing the effects of KK148, KK150 and epi-allopregnanolone (3β5αP) on maximal steady-state GABA-elicited currents. $\alpha_1\beta_3$ $GABA_ARs$ expressed in *Xenopus laevis* oocytes were activated with 1 mM GABA to maximally activate $GABA_AR$ current. (**A–C**) The effect of KK148 (10 μM), KK150 (10 μM) and 3β5αP (3 μM) on steady-state current. (**D**) The effect of 3β5αP (3 μM) on steady-state current in $\alpha_1\beta_3$ $GABA_ARs$ containing the α_1V256S mutation, known to eliminate NS-induced desensitization. The results show that 3β5αP and KK148 reduce steady-state currents, consistent with enhanced desensitization, whereas KK150 does not. The effect of 3β5αP on steady-state currents is eliminated by the α_1V256S mutation, consistent with 3β5αP enhancing desensitization rather than producing channel block.

The online version of this article includes the following figure supplement(s) for figure 2:

Figure supplement 1. Co-application of epi-allopregnanolone with a saturating concentration of GABA.

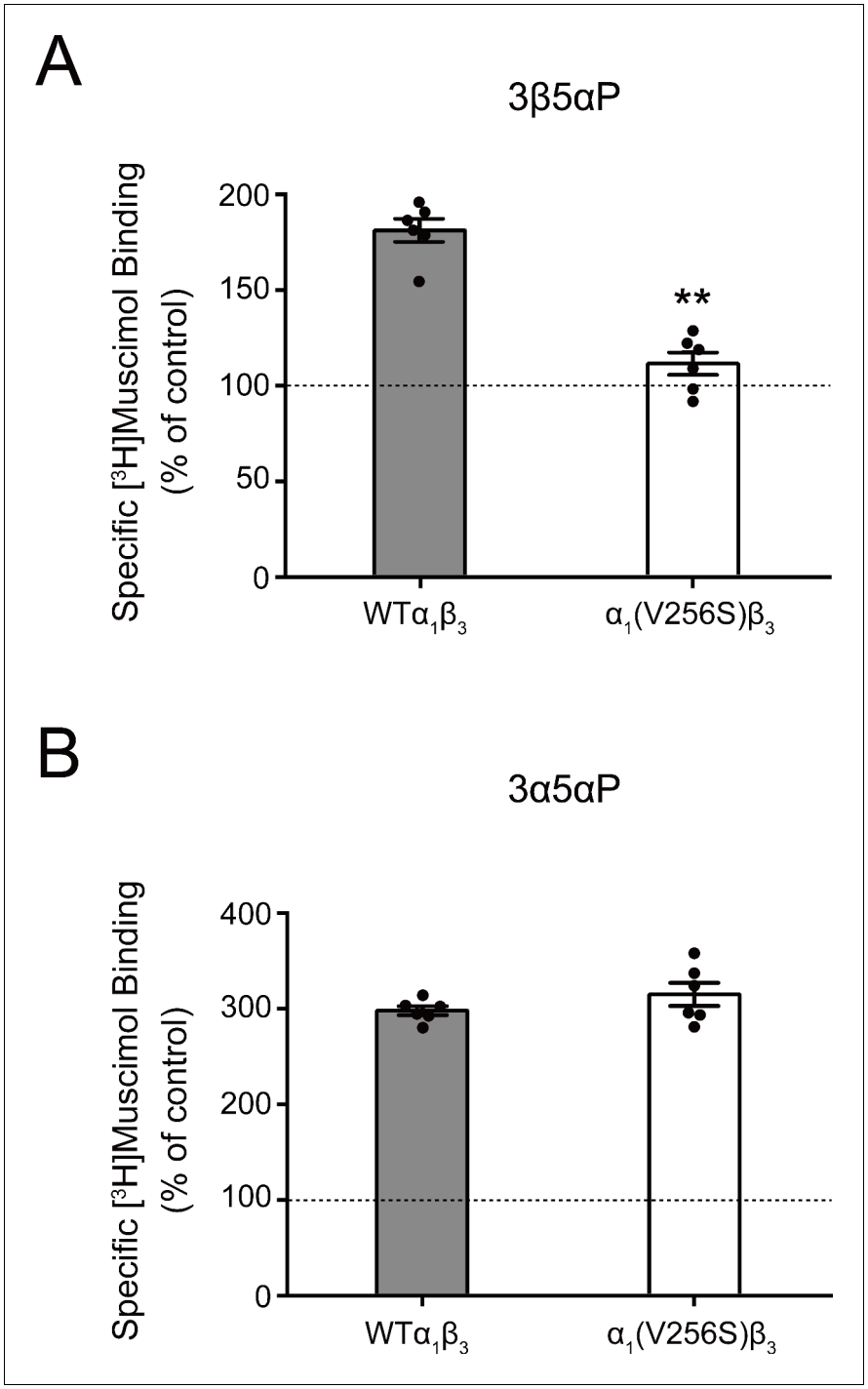

Figure 3. Effect of α_1(V256S)β_3 mutation on neurosteroid enhancement of [^{3}H]muscimol binding. (**A**) Enhancement of specific [^{3}H]muscimol (3 nM) binding to $\alpha_1\beta_3$ $GABA_AR$ WT by 10 µM epi-allopregnanolone (3β5αP) is absent in α_1(V256S)β_3 $GABA_AR$. (**B**) Enhancement of [^{3}H]muscimol binding by 10 µM allopregnanolone (3α5αP) is unaffected by the α_1V256S mutation. These data indicate that 3β5αP enhancement of orthosteric ligand binding requires receptor desensitization, whereas 3α5αP does not. Statistical differences are compared using unpaired *t*-test (*n* = 6,± SEM). **p<0.01 vs. WT.

The inhibitory effect of 3β5αP was not observed in receptors with the α_1(V256S) TM2 pore-lining mutation, which was previously shown to remove the inhibitory effects of sulfated steroids (***Akk et al., 2001***; ***Wang et al., 2002***; ***Figure 2D***). Although both 3α5αP and 3β5αP enhance [^{3}H]

muscimol binding, the former predominantly results in receptor activation, whereas the latter results in inhibition. Consistent with this, the α_1(V256S)β_3 mutation which abolishes NS-induced inhibition (**Akk et al., 2001**; **Wang et al., 2002**) eliminated [^{3}H]muscimol binding enhancement by 3β5αP but not 3α5αP (**Figure 3**). We infer that 3α5αP increases [^{3}H]muscimol binding by stabilizing an active state of the receptor. In contrast, 3β5αP increases [^{3}H]muscimol binding by stabilizing a desensitized state of the receptor; this effect is eliminated in the α_1(V256S)β_3 receptor. The mechanisms of enhancement of [^{3}H]muscimol binding by allosteric activators and inhibitors are described in detail in our recent publication (**Akk et al., 2020**). Collectively, these data indicate that 3β5αP and KK148 enhance orthosteric ligand affinity by stabilizing a desensitized state of the $GABA_AR$.

Quantitative comparison of the effects of 3β5αP on [^{3}H]muscimol binding and receptor desensitization

While there is qualitative agreement between the relative effects of the various NS analogues on orthosteric ligand binding and receptor desensitization, there is a quantitative discrepancy in the magnitude of the effects. For example, 3β5αP enhances [^{3}H]muscimol binding by two-fold (**Figure 1E**), whereas it reduces steady-state current by only ~25% (**Figure 2C**). To address this difference, we considered that the radioligand binding and electrophysiological assays are performed under different experimental conditions. The radioligand-binding studies are performed using low [^{3}H]muscimol concentrations to allow for sufficient dynamic range of ligand binding. In contrast, the desensitization experiments are performed at high orthosteric ligand (GABA) concentration to achieve high peak open probability and steady-state receptor desensitization, thus minimizing the number of channels in the resting state. To address the quantitative differences in results from the two assays, we analyzed the electrophysiological data in the framework of the three-state Resting-Open-Desensitized model (**Germann et al., 2019a**; **Germann et al., 2019b**). We assumed that both the open and desensitized states had higher affinity for muscimol than the resting state, and that the affinities were similar and could be treated as equal. We then calculated the predicted occupancy of the high-affinity states (P_{open} + $P_{desensitized}$) using parameters derived from the functional responses, to compare to the observed changes in binding. The raw current amplitudes of peak and steady-state responses were converted to units of open probability as described previously in detail (**Eaton et al., 2016**), and the probabilities of being in the open (P_{open}) or desensitized ($P_{desensitized}$) states were calculated for different experimental conditions (see Materials and methods).

Application of 1 mM GABA elicited a current response that had a peak P_{open} of 0.71 ± 0.25 (mean ± SD; n = 16). The P_{open} of the steady-state response was 0.121 ± 0.033 (n = 7), that was reduced to 0.077 ± 0.013 (n = 5) with 3 μM 3β5αP. Analysis of steady-state currents using the Resting-Open-Desensitized model indicates that the steady-state $P_{desensitized}$ is 0.829 in the presence of GABA, and 0.892 in the presence of GABA + steroid. The relatively small increase in the sum of (P_{open} + $P_{desensitized}$) (from 0.95 to 0.97) is due to the use of saturating GABA in these experiments.

To compare the data from the radioligand binding and electrophysiology experiments, we exposed oocytes containing $\alpha_1\beta_3$ $GABA_ARs$ to 20 nM muscimol and recorded currents before and after co-application of 3 μM 3β5αP. The percent reduction in steady-state current following 3β5αP exposure was measured and used to estimate the relative probabilities of resting, open and desensitized receptors. The application of 20 nM muscimol elicited a peak response with P_{open} of 0.012 ± 0.004 (n = 6). The steady-state P_{open} was 0.011 ± 0.004. In the same cells, subsequent exposure to 3 μM 3β5αP reduced the steady-state P_{open} to 0.009 ± 0.004 (p=0.0174; paired t-test). The calculated steady-state $P_{desensitized}$ was 0.1001 in the presence of muscimol, and 0.2168 in the presence of muscimol + 3β5αP. Thus, there is a predicted two-fold increase in the sum of (P_{open} + $P_{desensitized}$) when the steroid is combined with muscimol, consistent with the doubling of muscimol binding caused by 3β5αP in the [^{3}H]muscimol binding experiments (**Figure 1E**). While the measured changes in current are small, they are precise because each experiment served as its own control; a steady-state current was achieved during continuous agonist administration and the response to 3β5αP was then measured. Overall, these data indicate that when $P_{resting}$ is high (low orthosteric ligand concentration), an agent that stabilizes desensitized receptors may produce a small decrease in steady-state current, but a relatively large increase in the occupancy of desensitized state, at the expense of resting receptors. Conversely, with high orthosteric ligand concentrations (low $P_{resting}$), a desensitizing ligand produces a relatively larger change in steady-state current as open receptors

are converted to desensitized receptors with minimal effect on the sum occupancy of high-affinity states.

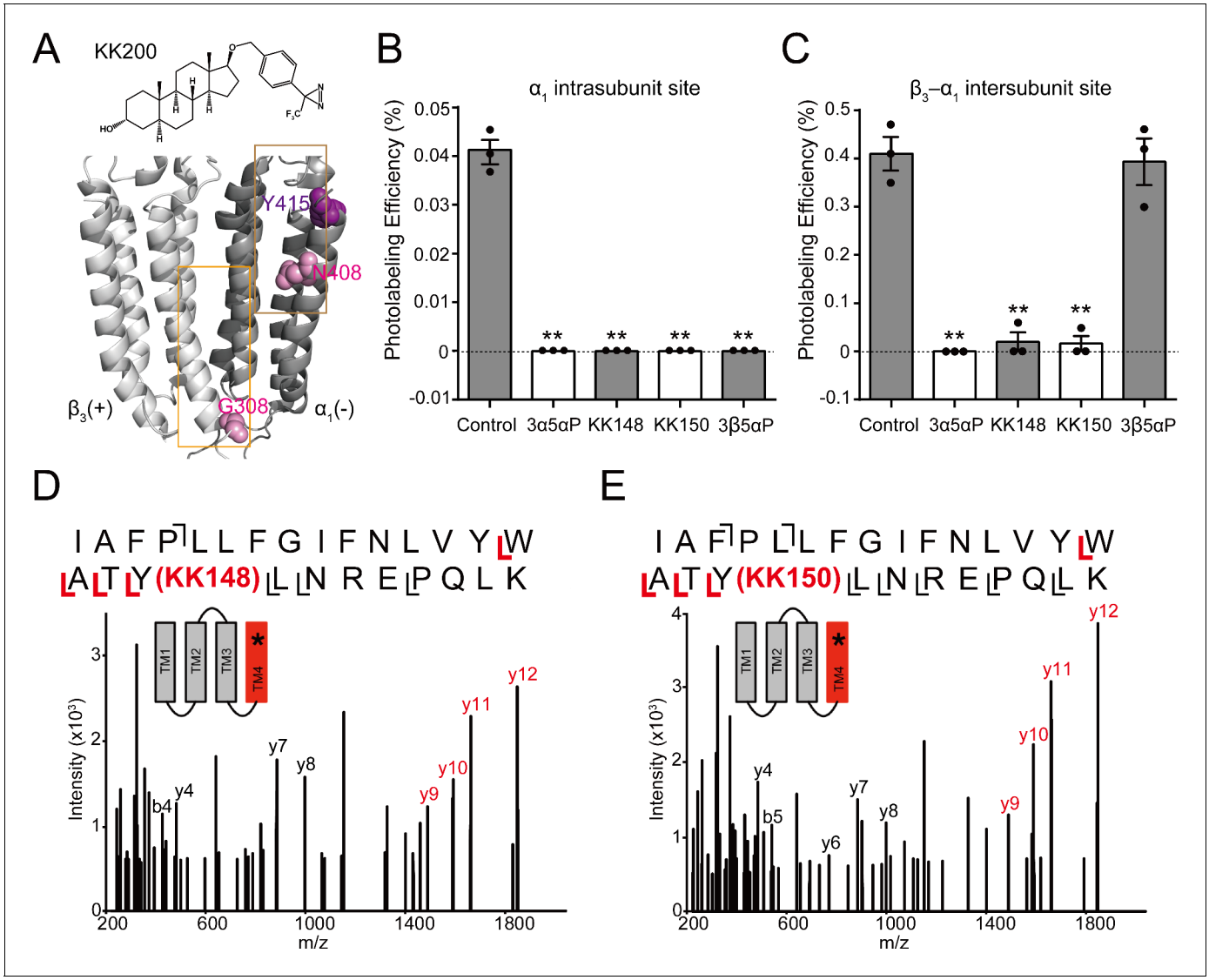

Figure 4. Competitive prevention of neurosteroid photolabeling at an intersubunit and intrasubunit site. (**A**) Structures of the neurosteroid photolabeling reagent KK200 and the $\alpha_1\beta_3$ $GABA_AR$-TMDs highlighting the residues G308 in the β_3(+)–α_1(-) intersubunit site and N408 in the α_1 intrasubunit site previously identified by KK200 photolabeling in pink. Shown in purple is Y415 in the α_1 intrasubunit site, which is photolabeled by KK148 and KK150. Adjacent β_3(+) and α_1(-) subunits are shown and the channel pore is behind the subunits. (**B**) Photolabeling efficiency of α_1 subunit TM4 (α_1 intrasubunit site) in $\alpha_1\beta_3$ $GABA_AR$ by 3 μM KK200 in the absence or presence of 30 μM allopregnanolone (3α5αP), KK148, KK150, and epi-allopregnanolone (3β5αP). Statistical differences are analyzed using one-way ANOVA with Bonferroni's multiple comparisons test (n = 3,± SEM). **p<0.01 vs. control. (**C**) Same as (**B**) for β_3 subunit TM3 [β_3(+)–α_1(-) intersubunit site, n = 3,± SEM]. (**D**) HCD fragmentation spectrum of the α_1 subunit TM4 tryptic peptide photolabeled by 30 μM KK148. Red and black indicate fragment ions that do or do not contain KK148, respectively. The schematic highlight in red identifies the TMD being analyzed and the asterisk denotes the approximate location of KK148. (**E**) Same as (**D**) photolabeled by 30 μM KK150.

The online version of this article includes the following figure supplement(s) for figure 4:

Figure supplement 1. Extracted ion chromatograms of labeled and unlabeled β_3 subunit TM4 peptides.

Figure supplement 2. Fragmentation spectrum of unlabeled α_1 subunit TM4 peptide.

Binding site selectivity for NS analogues

To determine whether KK148 and 3β5αP stabilize a desensitized conformation of the $GABA_AR$ by selectively binding to one or more of the identified NS-binding sites on the $GABA_AR$ (***Chen et al., 2019***), we first determined which of the identified NS sites they bind. We have previously shown that the 3α5αP-analogue photolabeling reagent, KK200 labels the β_3(+)–α_1(-) intersubunit (β_3G308) and α_1 intrasubunit (α_1N408) sites on $\alpha_1\beta_3$ $GABA_ARs$ (***Figure 4A***), and that photolabeling can be prevented by a 10-fold excess of 3α5αP (***Chen et al., 2019***). As a first step to determine the binding sites for 3β5αP, KK148 or KK150, we examined whether a 10-fold excess of these compounds (30 μM) prevented KK200 (3 μM) photolabeling of either binding site. Photolabeling was performed on membranes from HEK293 cells transfected with epitope-tagged $\alpha_{1His\text{-}FLAG}\beta_3$ receptors, mimicking

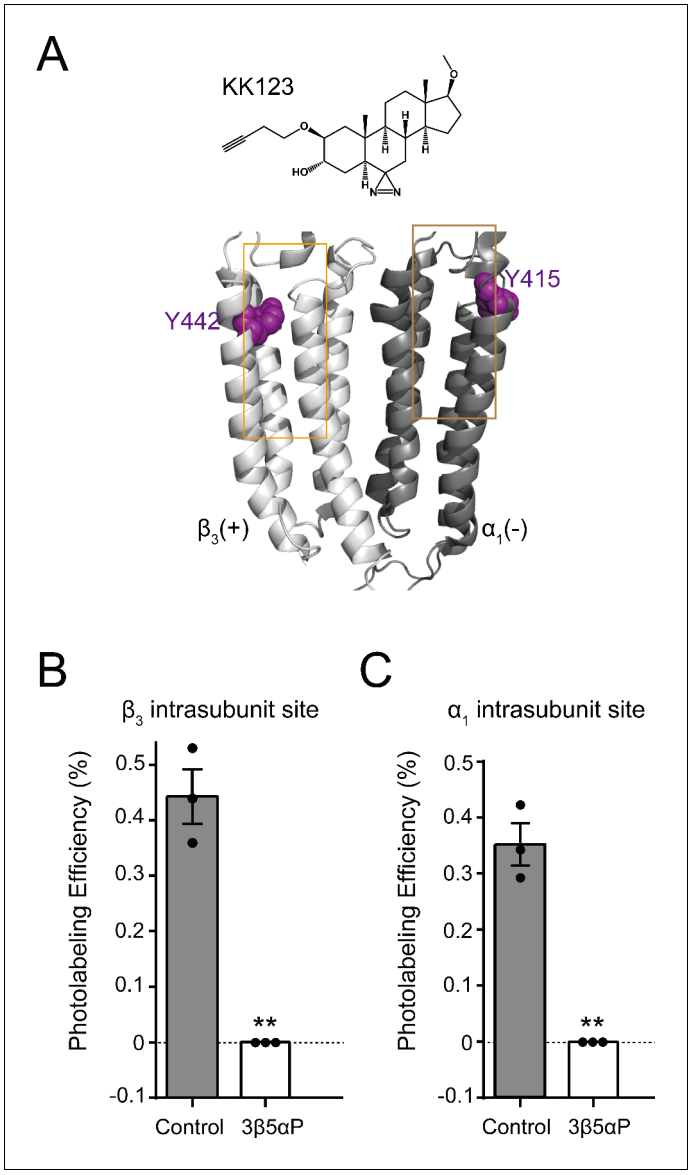

Figure 5. Epi-allopregnanolone prevents neurosteroid photolabeling at the α_1 and β_3 intrasubunit sites. (**A**) Structures of the neurosteroid photolabeling reagent KK123 and the $\alpha_1\beta_3$ $GABA_AR$-TMDs highlighting the residues Y442 in the β_3 intrasubunit site and Y415 in the α_1 intrasubunit site previously identified by KK123 photolabeling in purple. Adjacent β_3(+) and α_1(-) subunits are shown and the channel pore is behind the subunits. (**B**) Photolabeling efficiency of β_3 subunit TM4 (β_3 intrasubunit site) in $\alpha_1\beta_3$ $GABA_AR$ by 3 μM KK123 in the absence or presence of 30 μM epi-allopregnanolone (3β5αP). Statistical differences are compared using unpaired *t*-test (n = 3,± SEM). **p<0.01 vs. control. (**C**) Same as (**B**) for α_1 subunit TM4 (α_1 intrasubunit site, n = 3,± SEM).

the conditions used in the [^{3}H]muscimol binding assays and photolabeled residues were identified and labeling efficiency was determined using middle-down mass spectrometry (**Chen et al., 2019**). KK148, KK150, 3α5αP and 3β5αP all prevented KK200 photolabeling of α_1N408 in the α_1 intrasubunit site (**Figure 4B**), consistent with their binding to this site. In contrast, KK148, KK150 and 3α5αP but not 3β5αP prevented labeling of β_3G308 in the intersubunit site (**Figure 4C**), indicating that 3β5αP does not bind to the intersubunit site. Similarly, 3β5αP did not prevent labeling of the intersubunit site by a similar NS-analogue photolabeling reagent in detergent-solubilized $GABA_A$Rs (**Jayakar et al., 2020**).

The KK148- and KK150-photolabeled (30 μM) samples were also analyzed to directly identify the sites of adduction. In both the KK148- and KK150-labeled samples, photolabeled peptides were identified from the TM4 helices of both the α_1 and β_3 subunits. The labeled peptides had longer chromatographic elution times than the corresponding unlabeled peptides and corresponded with high mass accuracy (<20 ppm) to the predicted mass of the unlabeled peptides plus the add weight minus N_2 of KK148 or KK150 (**Figure 4—figure supplement 1**). Product ion (MS2) spectra of the KK148- and KK150-labeled peptides from the α_1 subunit identified the labeled residue as Y415 for both KK148 and KK150 with photolabeling efficiencies of 0.77% and 0.62%, respectively (**Figure 4D–E**, **Figure 4—figure supplement 2**); Y415 is the same residue labeled by KK123 at the α_1 intrasubunit site (**Chen et al., 2019**). The KK148 and KK150 labeled peptides in TM4 of the β_3 subunit and corresponding unlabeled peptide were identified by fragmentation spectra as β_3TM4 I426-N445. These data support labeling of the β_3 intrasubunit site by KK148 and KK150. Fragmentation spectra of the peptide-sterol adducts were not adequate to determine the precise labeled residue because of low photolabeling efficiency (0.13% for KK148; 0.19% for KK150, **Figure 4—figure supplement 1**). No photolabeled peptides were identified in the β_3(+)–α_1(-) intersubunit site. This is likely because KK148 and KK150, similar to KK123, utilize an aliphatic diazirine that preferentially labels nucleophilic residues (**Sugasawa et al., 2019**; **Budelier et al., 2017**; **Das, 2011**); such residues are not present in the intersubunit site.

We have also shown that KK123 labeling of the α_1 intrasubunit (α_1Y415) and β_3 intrasubunit (β_3Y442) sites (**Figure 5A**) can be prevented by a 10fold excess of 3α5αP (**Chen et al., 2019**). We thus examined whether 3β5αP (30 μM) inhibited photolabeling by KK123 (3 μM). 3β5αP completely inhibited KK123 photolabeling at both intrasubunit sites (**Figure 5B–C**). Collectively, the data show that KK148, KK150 and 3α5αP bind to all three of the identified NS-binding sites. In contrast, 3β5αP selectively binds to the two intrasubunit binding sites, but not to the canonical β_3(+)–α_1(-) intersubunit site.

Orthosteric ligand binding enhancement by NS analogues is mediated by distinct sites

To determine which of the previously identified binding sites contributes to NS enhancement of [^{3}H] muscimol binding, we performed site-directed mutagenesis of the NS-binding sites previously determined by photolabeling (**Figure 6A**; **Chen et al., 2019**). Specifically, α_1(Q242L)β_3 targets the β_3(+)–α_1(-) intersubunit site, α_1(N408A/Y411F)β_3 and α_1(V227W)β_3 the α_1 intrasubunit site, and $\alpha_1\beta_3$(Y284F) the β_3 intrasubunit site. None of these mutations produced a significant change in [^{3}H] muscimol K_d (**Figure 7B** and **Figure 7—source data 1**). Accordingly, concentration-dependent NS effects were assayed at a fixed concentration of [^{3}H]muscimol (3 nM; ~EC_5). It should be noted that earlier studies showed two-component binding curves for [^{3}H]muscimol in brain membranes, with NS causing an increase in the B_{max} of the high-affinity component (**Harrison and Simmonds, 1984**). In contrast, our results with expressed $\alpha_1\beta_3$ $GABA_A$Rs show a single-component [^{3}H]muscimol binding curve with NS producing an increase in muscimol affinity. Our results are similar to results reported with expressed $\alpha_1\beta_3\gamma_2$ $GABA_A$Rs, where allosteric modulators increased the affinity of a single-component [^{3}H]muscimol binding curve (**Dostalova et al., 2014**). Whether the complex [^{3}H]muscimol binding curves observed in brain is the result of heterogeneity of receptor subtypes or multiple states of the $GABA_A$R is unresolved.

Mutations in the β_3(+)–α_1(-) intersubunit and α_1 intrasubunit sites decreased 3α5αP enhancement of [^{3}H]muscimol binding by ~80%, while mutation of the β_3 intrasubunit site led to a small decrease (**Figure 6B**, **Table 1**). The residual enhancement of [^{3}H]muscimol binding observed in receptors with mutations in the intersubunit or α_1 intrasubunit site occurs at 10fold higher concentrations of 3α5αP than wild-type (WT) and receptors with mutations in the β_3 intrasubunit site (**Table 1**), suggesting

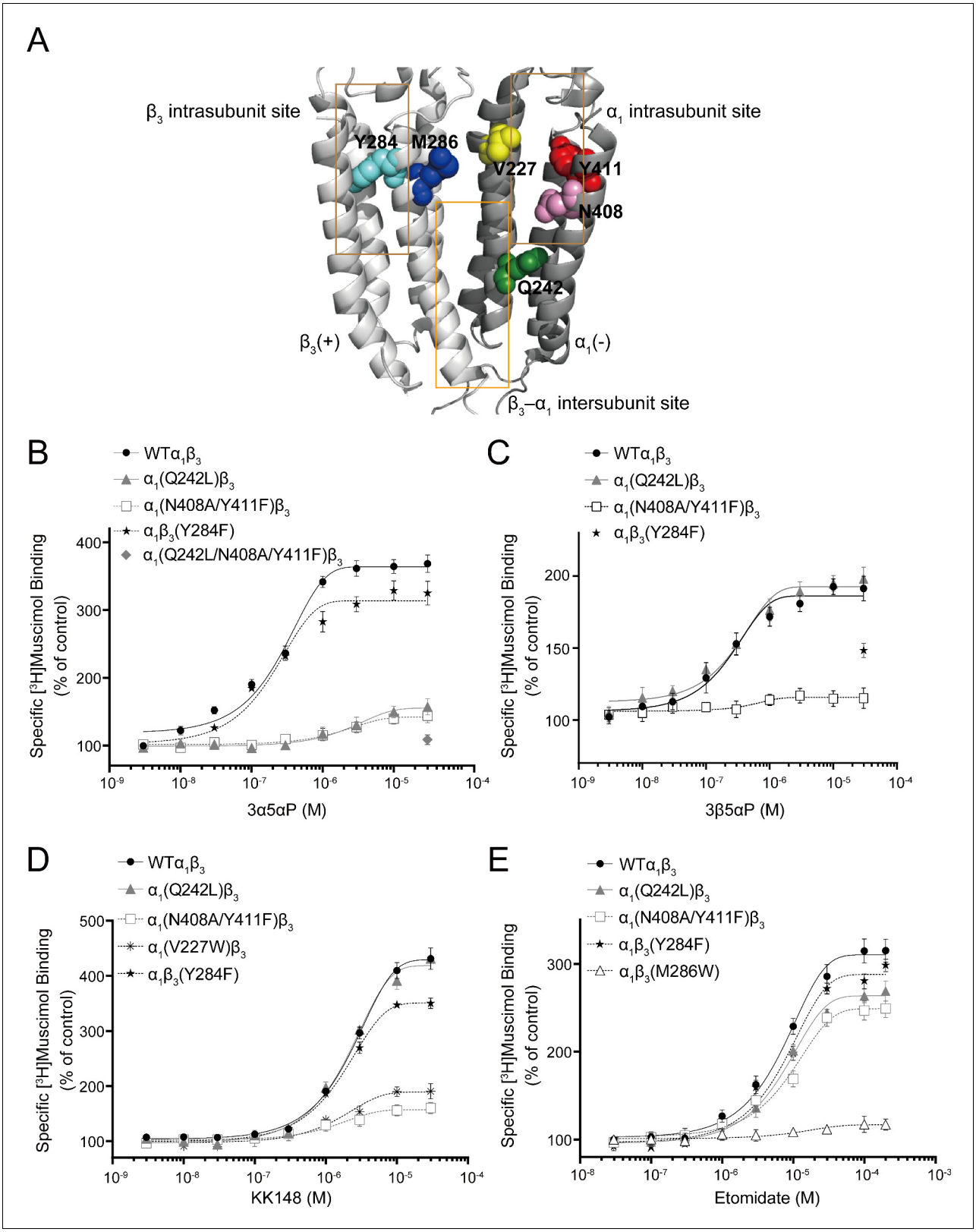

Figure 6. Effect of mutations in $\alpha_1\beta_3$ $GABA_AR$ on neurosteroid modulation of [^{3}H]muscimol binding. (**A**) Structure of the $\alpha_1\beta_3$ $GABA_AR$-TMD highlighting the residues where mutations were made in putative binding sites for neurosteroids (Q242-green for β_3–α_1 intersubunit site; V227-yellow, N408-pink and Y411-red for α_1 intrasubunit site; Y284-cyan for β_3 intrasubunit site) and M286-blue for etomidate. Adjacent β_3(+) and α_1(-) subunits are shown and the channel pore is behind the subunits. (**B**) Concentration-response relationship for the effect of 3 nM–30 μM allopregnanolone (3α5αP) on

Figure 6 continued on next page

Figure 6 continued

[^{3}H]muscimol (3 nM) binding to $\alpha_1\beta_3$ $GABA_AR$ WT and indicated mutants. Data points represent mean ± SEM (n = 6). (**C**), (**D**) and (**E**) Same as (**B**) for 3 nM–30 μM epi-allopregnanolone (3β5αP) (n = 3), KK148 (n = 6) and 30 nM–200 μM etomidate (n = 6), respectively. The data for WT in panels 6B and 6D is a replot of the same data shown in ***Figure 1E***.

The online version of this article includes the following figure supplement(s) for figure 6:

Figure supplement 1. Time course of neurosteroid modulation of muscimol binding.

that 3α5αP binds to the β_3 intrasubunit site with lower affinity. In contrast, mutations in the α_1 and β_3 intrasubunit sites, but not the intersubunit site decreased the enhancement of [^{3}H]muscimol binding by 3β5αP and KK148 (***Figure 6C–D***, ***Table 1***). To confirm that the effect of these mutations on NS effect are steroid-specific, we also tested their effect on etomidate, which enhances [^{3}H]muscimol binding in $\alpha_1\beta_3$ $GABA_ARs$ and acts through a binding site distinct from NS (***Li et al., 2006***; ***Jayakar et al., 2019***). The mutations targeting NS-binding sites resulted in modest decreases in [^{3}H]muscimol binding enhancement by etomidate; however, the $\alpha_1\beta_3$(M286W) mutation which abolishes etomidate potentiation and activation of $GABA_ARs$ (***Stewart et al., 2008***; ***Ziemba et al., 2018***), also abolished [^{3}H]muscimol binding enhancement (***Figure 6E***).

We did not test the effects of mutations on KK150 action because it minimally enhances [^{3}H]muscimol binding. However, KK150 binds to all three of the identified NS-binding sites, and may thus be a weak partial agonist or antagonist at the sites mediating NS enhancement of [^{3}H]muscimol binding. Consistent with this prediction, KK150 inhibited enhancement of [^{3}H]muscimol binding by 3α5αP and KK148 (***Figure 8***).

Collectively, these results show that multiple NS-binding sites contribute to enhancement of [^{3}H]muscimol affinity and that potentiating NS (3α5αP) and non-potentiating NS (3β5αP, KK148 and KK150) have both common and distinct sites of action. Specifically, 3α5αP enhances [^{3}H]muscimol binding through all three sites but predominantly through the intersubunit and α_1 intrasubunit sites, which we have previously shown mediate PAM-NS potentiation (***Chen et al., 2019***). In contrast, 3β5αP and KK148 enhance [^{3}H]muscimol binding exclusively through the α_1 and β_3 intrasubunit sites. KK150 antagonizes the effects of KK148 on [^{3}H]muscimol binding, presumably via the intrasubunit sites, and antagonizes the effects of 3α5αP, possibly via all three sites. These data indicate that NS binding to both the intersubunit and intrasubunit sites contributes to 3α5αP enhancement of [^{3}H]muscimol binding, but that only the intrasubunit binding sites contribute to the effects of 3β5αP and KK148. The data (***Figure 6B–D***) are consistent with NS producing their effects by independent action at each of the binding sites and our interpretation is based on that assumption. We cannot, however, rule out the possibility of an allosteric interaction between the NS binding sites (***Chen et al., 2019***).

It is important to note that the [^{3}H]muscimol binding curves in ***Figure 6*** are normalized to control. The raw data show that membranes containing WT receptors have 10–20-fold higher [^{3}H]muscimol binding (B_{max}) than membranes containing α_1(N408A/Y411F)β_3 receptors (***Figure 7A***), whereas the B_{max} of membranes containing α_1(Q242L)β_3, $\alpha_1\beta_3$(Y284F) or α_1(V227W)β_3 receptors was the same as for WT $\alpha_1\beta_3$ $GABA_ARs$ (***Figure 7—source data 1***). The lower total [^{3}H]muscimol binding observed in α_1(N408A/Y411F)β_3 membranes is likely a consequence of decreased receptor expression. To assure that differences in NS effect between WT and α_1(N408A/Y411F)β_3 are not due to different muscimol affinities, we examined [^{3}H]muscimol binding at a full range of concentrations. The α_1(N408A/Y411F)β_3 mutations did not have a significant effect on [^{3}H]muscimol affinity (***Figure 7B***), but eliminated the modulatory effects of NS (3α5αP and KK148) on [^{3}H]muscimol affinity (***Figure 7C–D*** and ***Figure 7—source data 2***). To assure that the effect of α_1(N408A/Y411F)β_3 was specific to NS, we also examined the effect of etomidate (a non-steroidal $GABA_AR$ PAM) on muscimol affinity. Etomidate enhanced [^{3}H]muscimol affinity in both the WT and α_1(N408A/Y411F)β_3 receptors, indicating that the effect of these mutations are specific to NS action (***Figure 7C–D***).

3β5αP increases desensitization through binding to α_1 and β_3 intrasubunit sites

To further explore the relationship between desensitization and enhancement of [^{3}H]muscimol binding, we examined the consequences of mutations to these sites on physiological measurements of desensitization induced by NS. Again, these experiments were performed with 3β5αP because it is

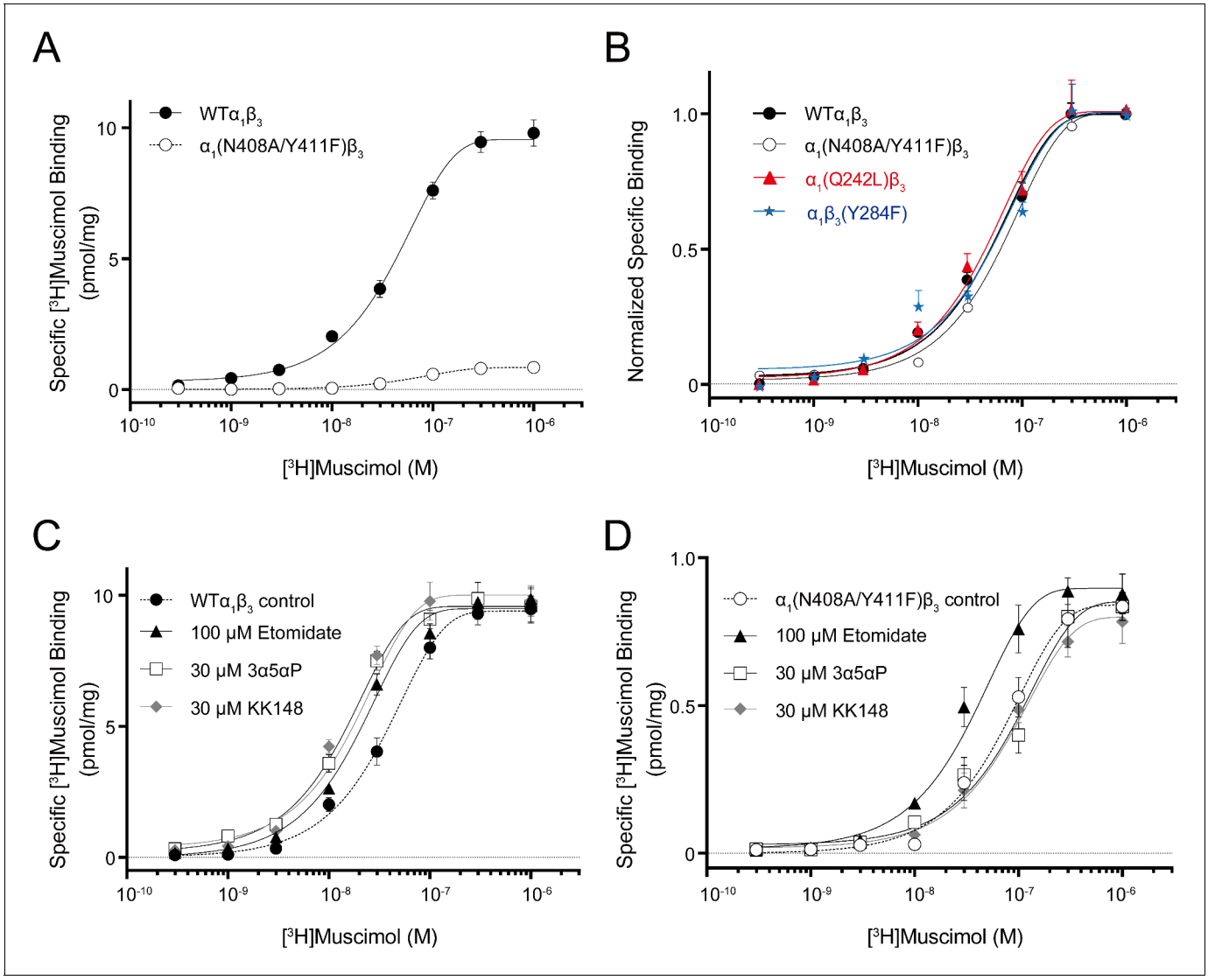

Figure 7. Neurosteroid effect on [^{3}H]muscimol binding isotherms in $\alpha_1\beta_3$ WT and α_1(N408A/Y411F)β_3 GABA$_A$Rs. (**A**) [^{3}H]muscimol binding isotherms (0.3 nM–1 μM) for $\alpha_1\beta_3$ GABA$_A$R WT and α_1(N408A/Y411F)β_3 GABA$_A$R. Data points are presented as mean ± SEM (n = 3). (**B**) Normalized curves of [^{3}H] muscimol binding isotherms (0.3 nM–1 μM) for $\alpha_1\beta_3$ GABA$_A$R WT and representative mutated receptors for each neurosteroid binding site [i.e. α_1(Q242L)β_3 for the β_3–α_1 intersubunit site; α_1(N408A/Y411F)β_3 for the α_1 intrasubunit site; $\alpha_1\beta_3$(Y284F) for the β_3 intrasubunit site]. Each data point represents mean ± SEM (n = 6 for WT; n = 3 for mutated receptors). (**C**) Effect of 100 μM etomidate, 30 μM allopregnanolone (3α5αP) and 30 μM KK148 on [^{3}H]muscimol binding isotherms in the $\alpha_1\beta_3$ GABA$_A$R WT. (**D**) Same as (**C**) in the α_1(N408A/Y411F)β_3 mutant. Each data point represents mean ± SEM (n = 3).

The online version of this article includes the following source data and figure supplement(s) for figure 7:

Source data 1. Properties of [^{3}H]muscimol binding isotherms in $\alpha_1\beta_3$ WT and mutant GABA$_A$Rs.
Source data 2. Properties of neurosteroid effect on [^{3}H]muscimol binding isotherms in $\alpha_1\beta_3$ GABA$_A$R WT and α_1(N408A/Y411F)β_3 mutant.
Figure supplement 1. Total, nonspecific and specific [^{3}H]muscimol binding curves.

the endogenous 3β-OH NS and because of limited quantities of KK148. Desensitization was quantified by defining the baseline steady-state current at 1 mM GABA as 100% and measuring percent reduction of the steady-state current elicited by a NS (***Figure 9A*** inset). While GABA was at a saturating concentration for all receptors, the peak P_{open} it elicited was <<1.0 for several of the mutated receptors. To normalize P_{open}, mutated receptors with low peak P_{open} were activated by co-application of 1 mM GABA with 40 μM pentobarbital (PB) (***Steinbach and Akk, 2001***) prior to application of 3α5αP. This was done because the magnitude of negative allosteric modulation varies as a function of P_{open} (***Germann et al., 2019a***). To ensure that PB did not influence NS negative allosteric

Table 1. Effects of mutations on neurosteroid modulation of [^{3}H]muscimol binding.
EC_{50}, Hill slope and maximal effect values [E_{max} (% of control): 100% means no effect] for the concentration-response curves in ***Figure 6B–E***. Statistical differences are analyzed using one-way ANOVA with Bonferroni's multiple comparisons test (*p<0.05 vs. WT; **p<0.01 vs. WT). Data are presented as mean ± SEM.

3α5αP	EC_{50} (μM)	Hill slope	E_{max} (% of control)	*N*
WT$\alpha_1\beta_3$	0.24 ± 0.04	1.10 ± 0.14	374.1 ± 11.1	6
α_1(Q242L)β_3	**2.66 ± 0.51	1.16 ± 0.37	**159.8 ± 10.9	6
α_1(N408A/Y411F)β_3	**2.30 ± 0.48	0.87 ± 0.44	**146.0 ± 9.3	6
$\alpha_1\beta_3$(Y284F)	0.19 ± 0.04	0.87 ± 0.16	342.3 ± 13.9	6
α_1(Q242L/N408A/Y411F)β_3	-	-	**105.9 ± 7.3	6
3β5αP				
WT$\alpha_1\beta_3$	0.25 ± 0.08	0.84 ± 0.23	195.1 ± 6.7	3
α_1(Q242L)β_3	0.27 ± 0.09	0.77 ± 0.21	204.3 ± 4.5	3
α_1(N408A/Y411F)β_3	0.61 ± 0.26	2.25 ± 0.92	**124.3 ± 2.6	3
$\alpha_1\beta_3$(Y284F)	-	-	**148.6 ± 4.9	3
KK148				
WT$\alpha_1\beta_3$	2.40 ± 0.36	1.36 ± 0.16	431.0 ± 19.5	6
α_1(Q242L)β_3	2.20 ± 0.31	1.24 ± 0.12	434.5 ± 5.6	6
α_1(N408A/Y411F)β_3	1.63 ± 0.53	0.73 ± 0.23	**161.7 ± 3.5	6
α_1(V227W)β_3	1.73 ± 0.68	0.76 ± 0.31	**209.2 ± 7.4	6
$\alpha_1\beta_3$(Y284F)	1.79 ± 0.44	1.35 ± 0.13	**357.2 ± 8.1	6
Etomidate				
WT$\alpha_1\beta_3$	7.24 ± 1.18	1.07 ± 0.17	331.1 ± 9.9	6
α_1(Q242L)β_3	7.50 ± 0.95	1.35 ± 0.20	**277.8 ± 10.9	6
α_1(N408A/Y411F)β_3	9.14 ± 2.20	1.07 ± 0.26	**268.2 ± 5.9	6
$\alpha_1\beta_3$(Y284F)	7.71 ± 1.10	0.90 ± 0.11	303.5 ± 5.8	6
$\alpha_1\beta_3$(M286W)	*22.5 ± 6.17	0.50 ± 0.16	**128.6 ± 7.8	6

modulation, control experiments were performed in WT $\alpha_1\beta_3$ $GABA_A$Rs and showed no significant difference in the desensitization elicited by 3β5αP between receptors activated by GABA vs. GABA plus PB. The maximum P_{open} for the mutant receptors varied between 0.55 and 0.95; some of the NS effects on macroscopic currents may be influenced by these differences.

3β5αP reduced the steady-state current (i.e. enhanced desensitization) by 23.0 ± 2.8% (% of desensitization: mean ± SEM, *n* = 5, ***Figure 9A***). Mutations in the α_1 and β_3 intrasubunit sites [i.e. α_1(N408A/Y411F)β_3 and $\alpha_1\beta_3$(Y284F), respectively] prevented 3β5αP-enhanced desensitization by ~67% (***Figure 9B***), whereas mutation in the β(+)–α(-) intersubunit site [α_1(Q242L)β_3] was without effect (***Figure 9B***). Receptors with mutations in both the α_1 and β_3 intrasubunit sites [α_1(N408A/Y411F)β_3(Y284F)] showed less NS-enhancement of desensitization than receptors with mutations in either of the intrasubunit sites alone, indicating that both intrasubunit sites contribute to the desensitizing effect (***Figure 9B***). Although the desensitizing effect of 3β5αP is completely eliminated by the V2'S mutation α_1(V256S)β_3, it is not completely eliminated by combined mutations of all three binding sites [α_1(Q242L/N408A/Y411F)β_3(Y284F)] (***Figure 9B***). This suggests either that the effects of the mutations are incomplete or there are additional unidentified NS-binding sites contributing to desensitization. Since mutations of the α_1 and β_3 intrasubunit sites also disrupt 3β5αP-enhancement of [^{3}H]muscimol binding (***Figure 6C***), we conclude that 3β5αP binding to these intrasubunit sites stabilizes the desensitized state of the $GABA_A$R and thus enhances [^{3}H]muscimol binding. Furthermore, KK148 increased $GABA_A$R desensitization (% of desensitization = 27.2 ± 6.0: mean ± SEM, *n* = 3, ***Figure 2A***) and the α_1(V256S)β_3 mutation abolished the effect (% of desensitization = 0, *n* = 1). These observations support the idea that binding of certain NS analogues to α_1 and β_3 intrasubunit

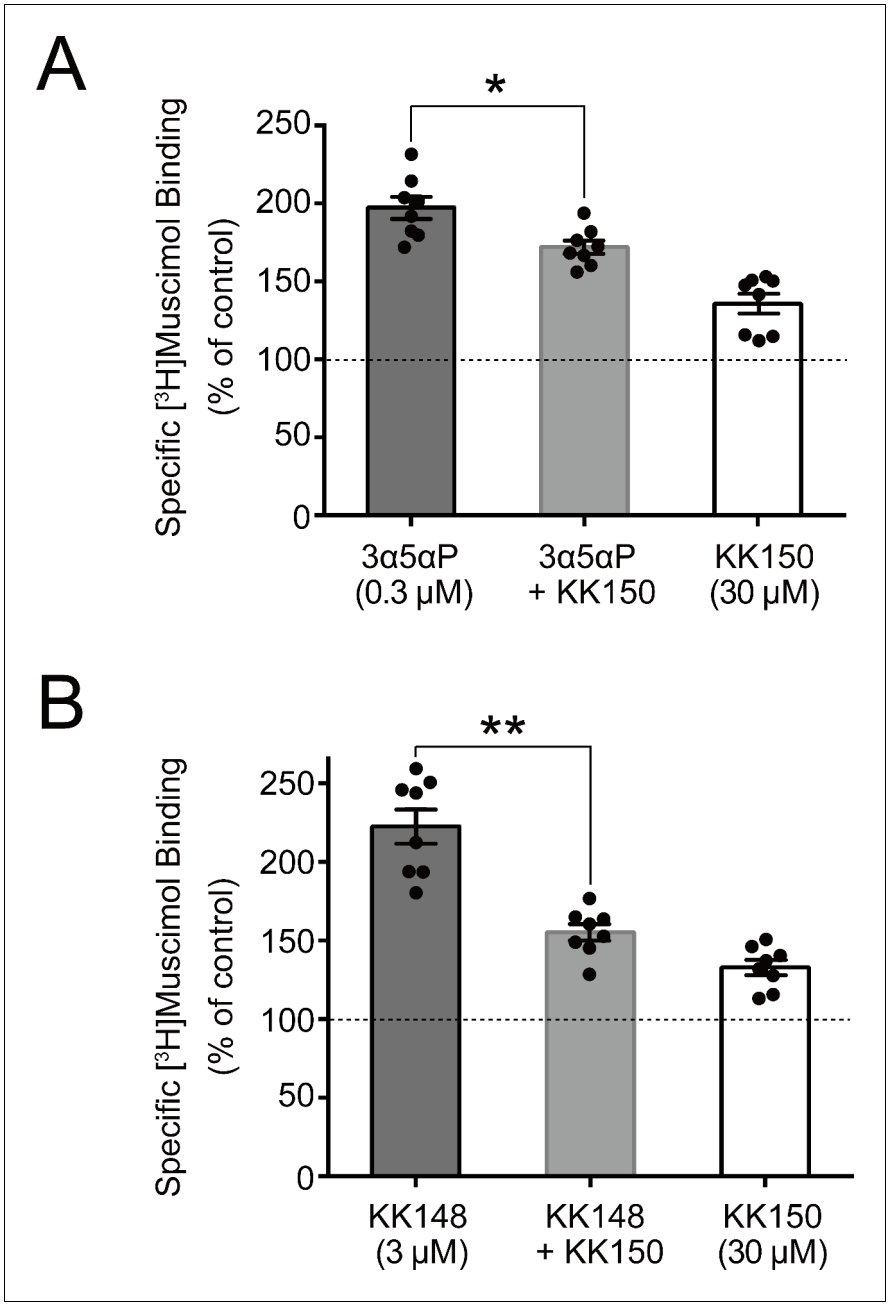

Figure 8. KK150 prevents neurosteroid-induced muscimol binding enhancement. (**A**) Enhancement of specific [^{3}H] muscimol (3 nM) binding to $\alpha_1\beta_3$ $GABA_AR$ by 0.3 μM allopregnanolone (3α5αP) in the absence (black bar) or presence (grey bar) of 30 μM KK150 and KK150 alone (white bar). Statistical differences are analyzed using one-way ANOVA with Bonferroni's multiple comparisons test (n = 8,± SEM). *p<0.05 vs. 0.3 μM 3α5αP alone. (**B**) Same as (**A**) for 3 μM KK148 (n = 8,± SEM). **p<0.01 vs. 3 μM KK148 alone.

sites, increases $GABA_AR$ desensitization. In contrast, KK150 showed a very small effect on desensitization (% of desensitization = 2.1 ± 0.7: mean ± SEM, n = 5, ***Figure 2B***), consistent with the small increase in [^{3}H]muscimol binding by KK150 (***Figure 1E***).

The effects of 3α5αP binding to intrasubunit sites on desensitization

3α5αP binds to all three of the NS-binding sites on $\alpha_1\beta_3$ $GABA_AR$, and mutations in all three sites reduce 3α5αP enhancement of [^{3}H]muscimol binding (***Figure 6B***). This suggests the possibility that activation by 3α5αP (mediated primarily by the β_3(+)–α_1(-) intersubunit site) masks a desensitizing

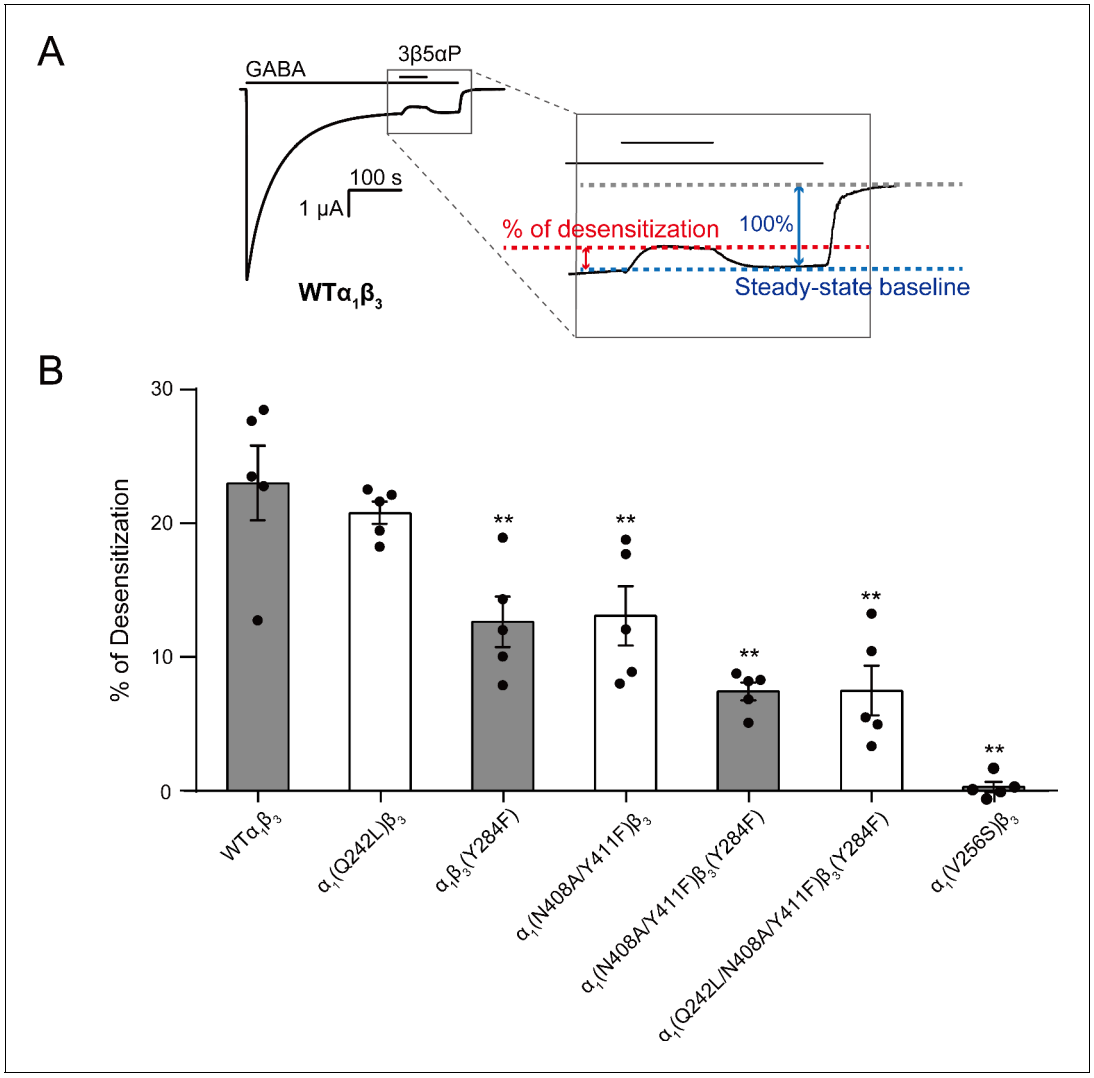

Figure 9. Mutations in intrasubunit sites prevent desensitization by epi-allopregnanolone. (**A**) Sample current trace showing the effect of 3 μM epi-allopregnanolone (3β5αP) on steady-state current elicited by continuous administration of 1 mM GABA to $\alpha_1\beta_3$ $GABA_AR$ expressed in oocytes. A zoomed-in box shows neurosteroid-induced desensitization of the steady-state GABA current. (**B**) Percent desensitization of the steady-state $\alpha_1\beta_3$ $GABA_AR$ currents (WT and mutants) by 3 μM 3β5αP during continuous application of 1 mM GABA [for WT, α_1(Q242L)β_3, $\alpha_1\beta_3$(Y284F), α_1(N408A/Y411F)β_3 and α_1(V256S)β_3 $GABA_ARs$] or 1 mM GABA + 25 μM pentobarbital (PB) [for α_1(N408A/Y411F)β_3(Y284F) and α_1(Q242L/N408A/Y411F)β_3(Y284F) $GABA_ARs$]. The combination of GABA and PB is essential for some mutated receptors to obtain a high, consistent peak open probability. Statistical differences are analyzed using one-way ANOVA with Bonferroni's multiple comparisons test (n = 5,± SEM). **p<0.01 vs. WT.

effect mediated through the β_3 and/or α_1 intrasubunit binding sites. To determine whether intrasubunit binding sites mediate increased desensitization by 3α5αP, we examined the effect of 3α5αP on steady-state currents in receptors with mutations in the α_1 or β_3 intrasubunit site. Mutations in the intrasubunit sites were prepared with a background α_1(Q242L)β_3 mutation to remove 3α5αP activation (***Chen et al., 2019***; ***Sugasawa et al., 2019***; ***Akk et al., 2008***; ***Bracamontes and Steinbach, 2009***) and focus on the effects of 3α5αP on the equilibrium between the open and desensitized states.

3α5αP produced a small reduction in steady-state current in α_1(Q242L)β_3 receptors with mutations in neither of the intrasubunit sites (***Figure 10A***). This inhibitory effect was eliminated by α_1(V256S)β_3, indicating that it was due to receptor desensitization (***Figure 10D***). In receptors with combined mutations in the intersubunit and α_1 intrasubunit sites [i.e. α_1(Q242L/N408A/Y411F)β_3], 3α5αP significantly inhibited the steady-state current (***Figure 10B***), an effect that was markedly reduced by mutations in the β_3 intrasubunit site [α_1(Q242L)β_3(Y284F)] (***Figure 10C***). These data

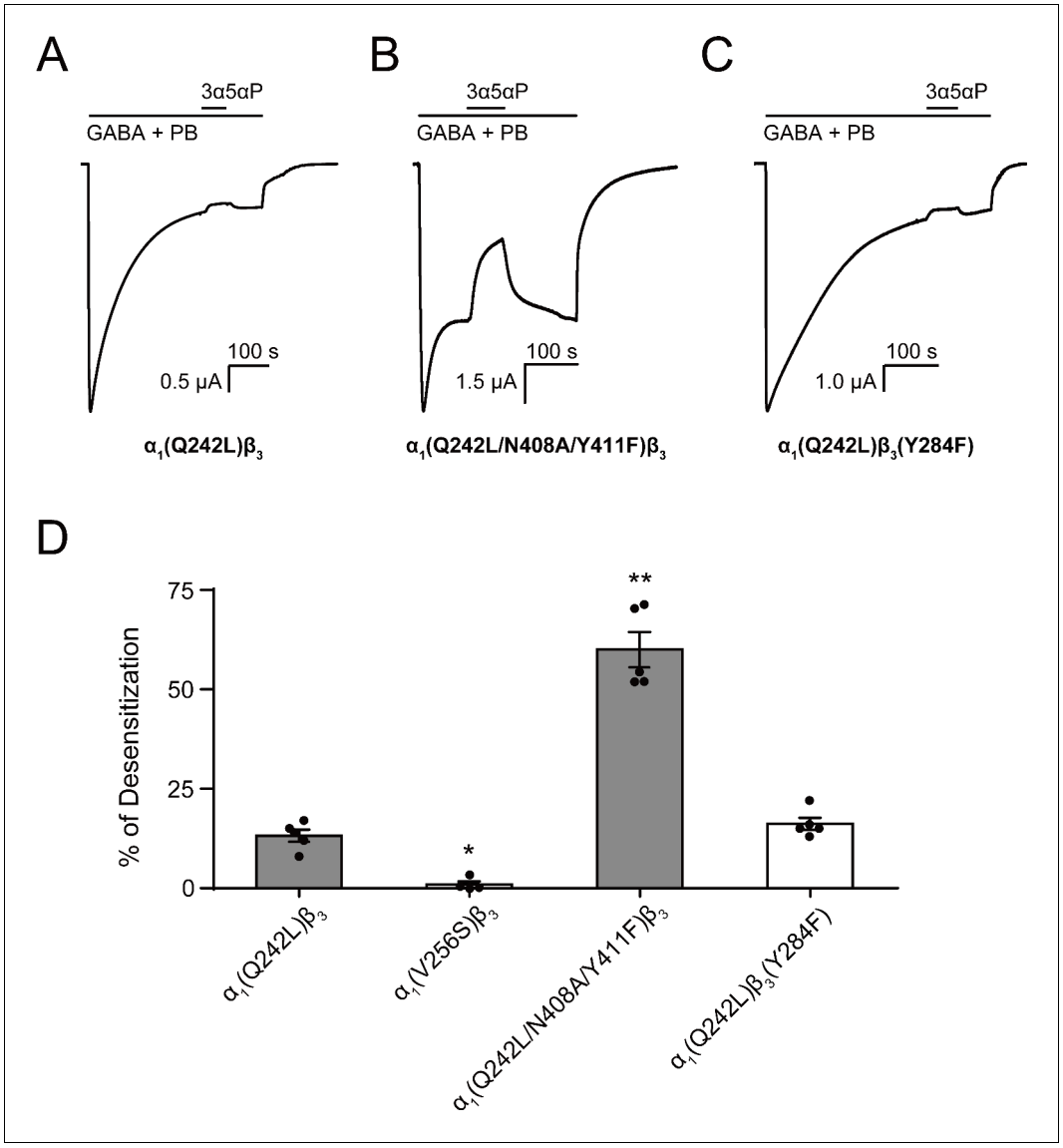

Figure 10. Allopregnanolone desensitizes $GABA_AR$ currents via binding to the β_3 intrasubunit site. (**A**) Sample current trace showing the effect of 3 μM allopregnanolone (3α5αP) on $\alpha_1(Q242L)\beta_3$ $GABA_AR$ activated by 1 mM GABA co-applied with 40 μM pentobarbital (PB). (**B**), (**C**) Same as (**A**) for $\alpha_1(Q242L/N408A/Y411F)\beta_3$ $GABA_AR$ and $\alpha_1(Q242L)\beta_3(Y284F)$ $GABA_AR$, respectively. (**D**) Percent desensitization of the steady-state currents elicited by 1 mM GABA with 40 μM PB in $\alpha_1\beta_3$ $GABA_AR$ with specified mutations. Statistical differences are analyzed using one-way ANOVA with Bonferroni's multiple comparisons test [n = 4 for $\alpha_1(V256S)\beta_3$; n = 5 for others,± SEM]. *p<0.05; **p<0.01 vs. $\alpha_1(Q242L)\beta_3$, respectively.

suggest that 3α5αP exerts a desensitizing effect by binding to the β_3 intrasubunit site and that 3α5αP binding to the α_1 intrasubunit site does not promote desensitization (***Figure 10D***). Notably, 3α5αP exerted only a modest inhibitory effect in $\alpha_1(Q242L)\beta_3$ receptors in which occupancy of the β_3 intrasubunit site should promote inhibition. This may be due to a counterbalancing action at the α_1 intrasubunit site, where 3α5αP binding contributes more to receptor activation as demonstrated by our previous observation that mutations in the α_1 intrasubunit site significantly reduce 3α5αP potentiation of GABA-elicited currents (***Chen et al., 2019***). These results suggest that in addition to activation, 3α5αP enhances receptor desensitization. Enhanced desensitization by the PAM-NS 3α5αP (***Haage and Johansson, 1999***) and 3α5α-THDOC (***Zhu and Vicini, 1997***; ***Bianchi and Macdonald, 2003***) has been observed in prior studies supporting the current finding with 3α5αP.

Discussion

In this study, we examined how site-specific binding to the three identified NS sites on $\alpha_1\beta_3$ $GABA_AR$ (**Chen et al., 2019**) contributes to the PAM vs. NAM activity of epimeric 3-OH NS. We found that the PAM-NS 3α5αP, but not the NAM-NS 3β5αP, binds to the canonical β_3(+)–α_1(-) intersubunit site that mediates receptor potentiation, explaining the absence of 3β5αP PAM activity. In contrast, 3β5αP binds to intrasubunit sites in the α_1 and β_3 subunits, promoting receptor desensitization. Binding to the intrasubunit sites provides a mechanistic explanation for the NAM effects of 3β5αP (**Wang et al., 2002**). 3α5αP also binds to the β_3 intrasubunit site explaining the previously described desensitizing effect of the PAM-NS 3α5αP (**Haage and Johansson, 1999**) and 3α5α-THDOC (**Zhu and Vicini, 1997**; **Bianchi and Macdonald, 2003**). Two synthetic NS with diazirine moieties at C3 (KK148 and KK150) were used to identify NS-binding sites and shown to bind to the intersubunit as well as both intrasubunit sites. Neither of these ligands potentiated agonist-activated $GABA_AR$ currents, reinforcing the importance of the 3α-OH group and its interaction with α_1Q242 in PAM actions. KK148 is an efficacious desensitizing agent, acting through the α_1 and β_3 intrasubunit NS-binding sites. KK150, the 17α-epimer of KK148, binds to all three NS-binding sites, but neither activates nor desensitizes $GABA_ARs$, suggesting a potential chemical scaffold for a general NS antagonist. Collectively, these data show that differential occupancy of and efficacy at three discrete NS-binding sites determines whether a NS ligand has PAM, NAM, or potentially NS antagonist activity on $GABA_ARs$.

The observation that 3β5αP and KK148 enhance orthosteric ligand binding but do not potentiate GABA-elicited currents first suggested that these NAM-NS selectively stabilize a non-conducting state that has high affinity to the orthosteric agonist muscimol. This liganded/closed state could represent a pre-active (**Gielen and Corringer, 2018**) or a desensitized conformation of the receptor (n.b. there may be multiple desensitized conformations of the receptor, possibly including NS-specific desensitized states). Chang and colleagues have shown that orthosteric ligand affinity (muscimol or GABA) is greater in desensitized and activated (open) $GABA_ARs$ than in resting (closed) receptors, with estimated GABA K_d values of 78.5 μM, 120 nM and 40 nM for the resting, activated and desensitized $\alpha_1\beta_2\gamma_2$ receptors respectively (**Chang et al., 2002**). Kinetic models also predict that a pre-active state should have higher affinity for an orthosteric agonist than the resting state (**Gielen and Corringer, 2018**). To distinguish between stabilization of a pre-active and a desensitized state, we co-applied 3β5αP with a high concentration of GABA. 3β5αP reduced the desensitization time constant but did not reduce peak current amplitude. While this result is consistent with stabilization of a desensitized rather than a pre-active state, it is ambiguous as it could also be explained by NAM-NS having a slower onset of effect than GABA because of slow access of the steroid to its binding site (**Li et al., 2007**). However, this result is supported by studies examining inhibitory postsynaptic currents (IPSCs) in which a NAM-NS can be pre-applied and the GABA concentration step is extremely rapid as well as by single channel studies. In cultured hippocampal neurons, the NAM-NS 3β5β-THDOC significantly reduced IPSCs decay times but had no effect on IPSCs amplitude, consistent with a desensitizing effect (**Wang et al., 2002**). Single channel analyses provide the most definitive distinction between a pre-active and a desensitized state. Desensitization is predicted to shorten single channel clusters without affecting intracluster open or closed time distributions. In contrast, steroid-induced stabilization of a pre-active non-conducting state may be expected to lead to increased mean intracluster closed time. Single-channel studies examining the kinetic effects of the inhibitory steroids pregnenolone sulfate (**Akk et al., 2001**) or the 3β5αP analogue (3β,5α,17β)−3-hydroxyandrostane-17-carbonitrile (3β5α-ACN) (Akk, G.; unpublished data) have indeed observed reduced mean cluster duration with minimal changes in intracluster open and closed time properties, indicative of the steroids promoting receptor desensitization. The α_1V256S mutation eliminated the PS-mediated reduction in cluster duration indicating that the mutation prevents PS-mediated desensitization (**Akk et al., 2001**). 3β-hydroxy steroids act similarly to PS, including exhibiting sensitivity to the α_1V256S mutation (**Wang et al., 2002**). Overall, the preponderance of evidence indicates that 3β-NAM-NS such as 3β5αP inhibit $GABA_AR$ currents by stabilizing a desensitized state.

Our experimental and modeling data demonstrate that NAM-NS such as 3β5αP or KK148 enhance orthosteric ligand binding by increasing the population of receptors in a desensitized state. It is, however, unclear if 3β5αP or KK148 can promote transition of resting receptors directly to a desensitized state, thus bypassing channel opening. We propose that in the presence of low

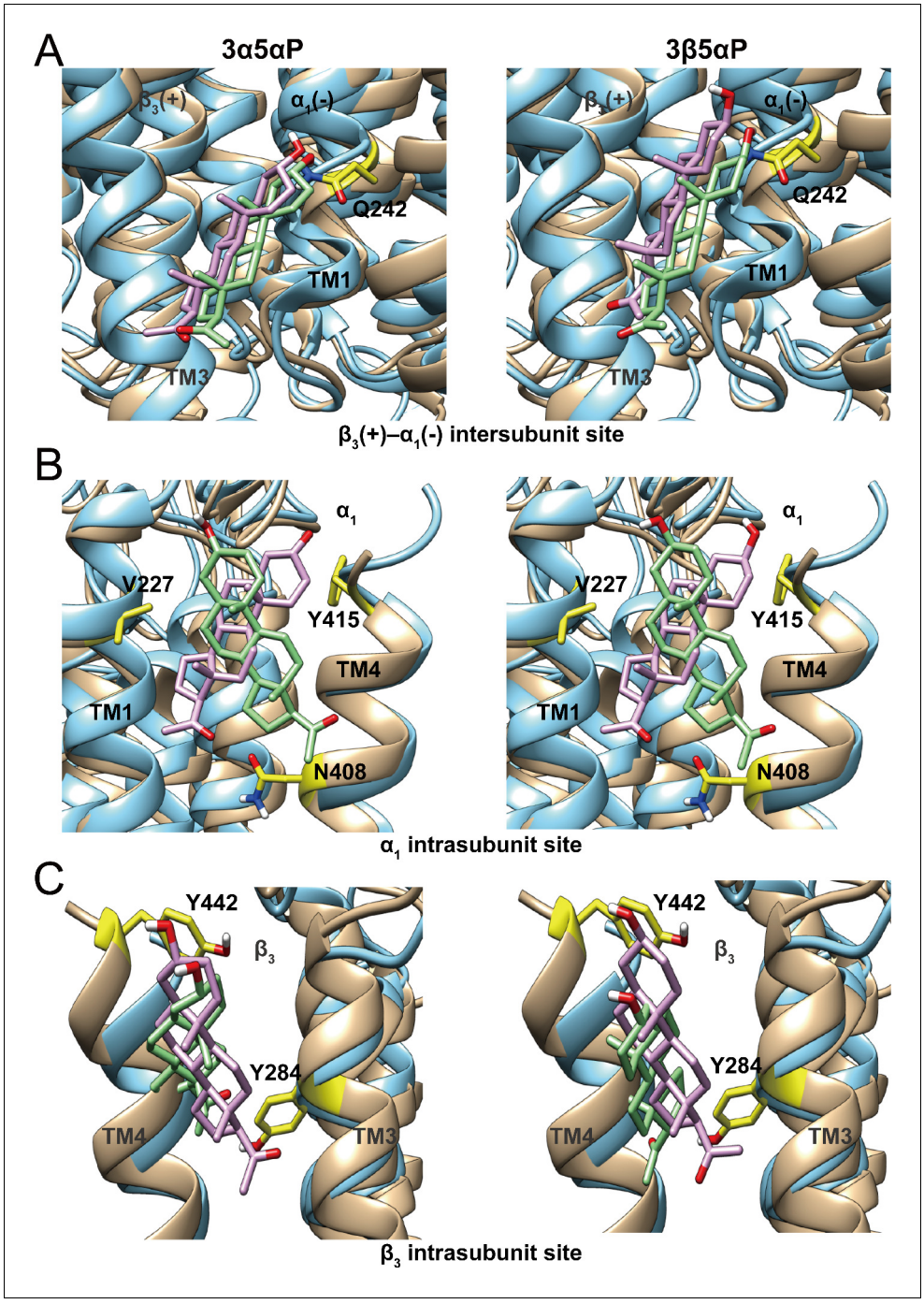

Figure 11. Comparison of allopregnanolone and epi-allopregnanolone docking poses within three neurosteroid binding pockets of the modeled $\alpha_1\beta_3$ $GABA_AR$ TMD and the cryo-EM structure of an $\alpha_1\beta_3\gamma_2$ $GABA_AR$ (PDB ID: 6I53). The two structures were read into UCSF Chimera and mutually aligned using MatchMaker. The $\alpha_1\beta_3$ model is shown in tan, while the $\alpha_1\beta_3\gamma_2$ structure is in cyan. (**A**) Representative poses for allopregnanolone (3α5αP) and epi-allopregnanolone (3β5αP) docked within the β_3(+)–α_1(-) intersubunit site, the poses for the $\alpha_1\beta_3$ model are in pink, while those for the $\alpha_1\beta_3\gamma_2$ structure are in light green. The α_1Q242 side chain is shown in yellow. (**B**) Same as for (**A**) for the α_1 intrasubunit site; also shown are the sidechains V227, Y415, and N408. (**C**) Same as (**A**) for the β_3 intrasubunit site; also shown are the sidechains Y284 and Y442. The Vina docking scores for 3α5αP and 3β5αP at each site in the $\alpha_1\beta_3$ model and the $\alpha_1\beta_3\gamma_2$ structure are shown in ***Figure 11—source data 1***.
The online version of this article includes the following source data for figure 11:

Source data 1. Vina docking scores for allopregnanolone and epi-allopregnanolone at each site in $\alpha_1\beta_3$ model and $\alpha_1\beta_3\gamma_2$ $GABA_AR$ structure.

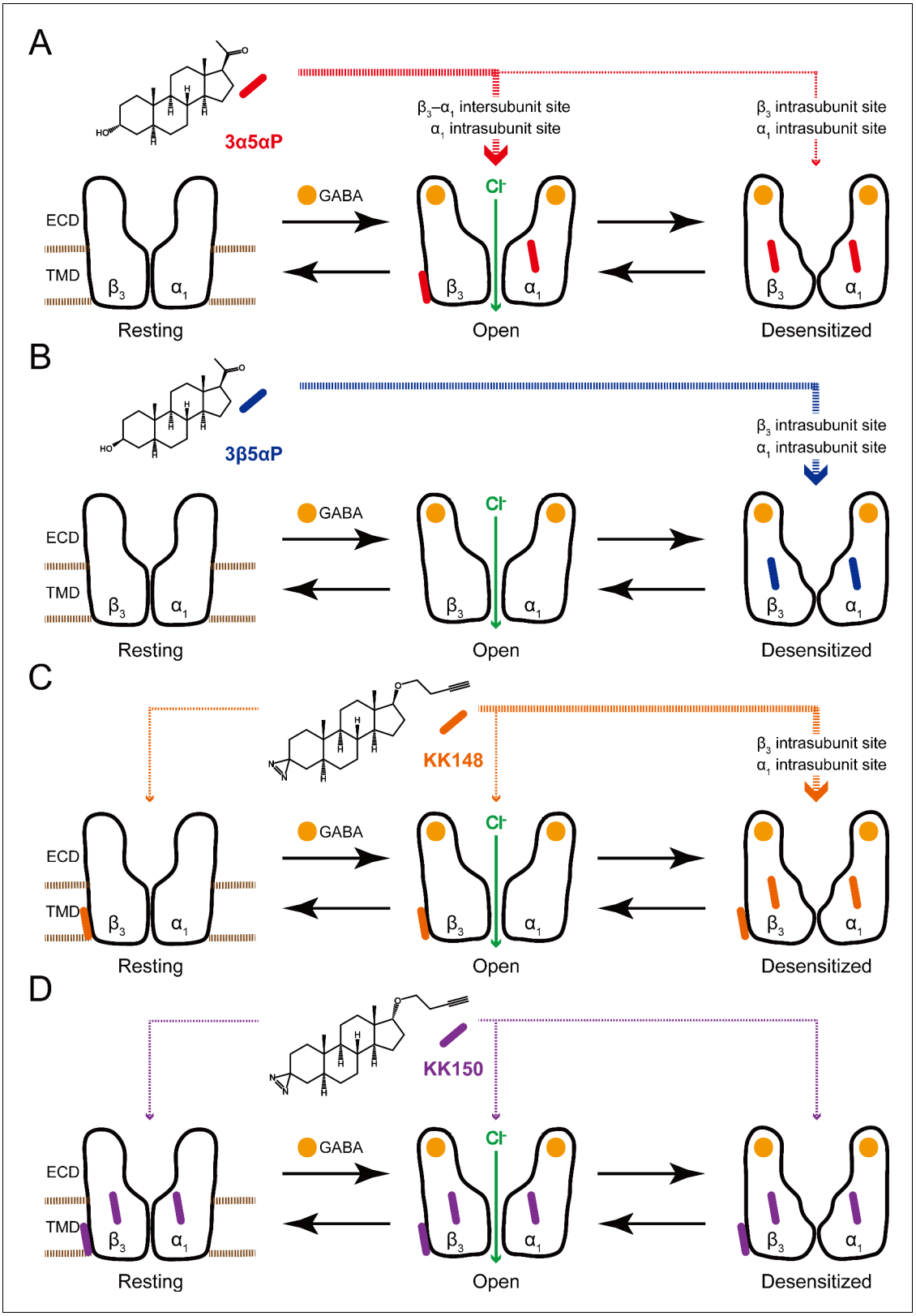

Figure 12. Neurosteroids preferentially stabilize $GABA_AR$ in different states. (**A**) Model showing three fundamental conformational states that depict the channel function in the $GABA_AR$: a resting state; an open state; and a desensitized state. Agonist (GABA:) binding shifts the equilibrium towards high-affinity states (open and desensitized). Allopregnanolone (3α5αP:) allosterically stabilizes the high-affinity states (an open state through the β_3–α_1 intersubunit and the α_1 intrasubunit sites; a desensitized state through the β_3 intrasubunit site). The width of red arrows indicates relative affinities of

Figure 12 continued on next page

Figure 12 continued

3α5αP for the open or desensitized state of the receptor. (**B**) Same as (**A**) for epi-allopregnanolone (3β5αP:). 3β5αP stabilizes a desensitized state through the β_3 and α_1 intrasubunit sites. (**C**) Same as (**A**) for KK148 ( ). KK148 allosterically stabilizes a desensitized state through the β_3 and α_1 intrasubunit sites, and equally stabilizes all three states of the receptor through the β_3–α_1 intersubunit site. The width of orange arrows indicates relative affinities of KK148 for each state of the receptor. (**D**) Same as (**A**) for KK150 ( ). KK150 equally stabilizes all three states of the receptor through the β_3 and α_1 intrasubunit sites, and the β_3–α_1 intersubunit site.

concentrations of orthosteric agonists (as in the [^{3}H]muscimol binding assays), there is a slow shift of receptors from resting through activated to a desensitized state with minimal change in the population of receptors in the activated state. The slow time course of accumulation of desensitized receptors is illustrated by experiments in which 10 μM 3β5αP is added to membranes that have been fully equilibrated with a low concentration (3 nM) of [^{3}H]muscimol and binding is measured as a function of time. Enhancement of [^{3}H]muscimol binding by 10 μM 3β5αP is slow, with a time constant of 4 min at 4˚C (τ = 3.97 ± 0.15 min: mean ± SEM, *n* = 4, ***Figure 6—figure supplement 1***). In contrast, when $\alpha_1\beta_3$ $GABA_A$Rs are exposed to long pulses of a high concentration of GABA, KK148- and 3β5αP-induced desensitization is rapid (***Figure 2A and C***), since in these conditions almost all of the receptors are either in an open or desensitized conformation and desensitization is not slowed by the transition from resting to open state (***Jones and Westbrook, 1995***). Thus, the slow enhancement of [^{3}H]muscimol binding by 3β5αP (***Figure 6—figure supplement 1***) is likely rate-limited by the transition of receptors to activated then to desensitized states at 3 nM muscimol rather than by 3β5αP binding. These time course experiments are most consistent with a model in which receptors preferentially progress from the resting to active to desensitized states, which are then stabilized by the NAM-NS.

The selective binding of 3β5αP to a subset of identified NS-binding sites provides an explanation for its NAM activity. 3β5αP stabilizes desensitized receptors by binding to the α_1 and β_3 intrasubunit sites, but does not activate the receptor because it does not bind to the intersubunit site. This site-selective binding is unexpected for several reasons. First, docking and free energy perturbation calculations in a prior study predicted that 3β5βP binds to the intersubunit site in a similar orientation and with free energies of binding that are equivalent to pregnanolone (3α5βP) (***Miller et al., 2017***). The modeling suggested that 3β5βP does not form a hydrogen bond with αQ242, a possible explanation for its lack of efficacy (***Miller et al., 2017***). Our docking studies also show similar binding energies and orientations of 3β5αP and 3α5αP binding in the β_3(+)–α_1(-) intersubunit site of either a homology model of the $\alpha_1\beta_3$ receptor or the cryo-EM structure (PDB ID: 6I53) of the $\alpha_1\beta_3\gamma_2$ receptor in a lipid nanodisc (***Laverty et al., 2019***; ***Figure 11***). We have also shown that binding affinity or docking scores of NS binding to the intersubunit site are not significantly affected by mutations (α_1Q242L, α_1Q242W, α_1W246L) that eliminate NS activation, although binding orientation is altered (***Sugasawa et al., 2019***). These data indicate that NS binding in the intersubunit site is tolerant to significant changes in critical residues and NS ligand structure, and are consistent with our findings that NS analogues, such as KK148 and KK150, can bind to the intersubunit site but have no effect on activation (***Figures 1*** and ***4***). Thus, the peculiar lack of 3β5αP binding to the intersubunit site suggests that either: (1) details in the structure of the intersubunit site in the open conformation that explain the absence of 3β5αP binding are not apparent in current high-resolution structures or; (2) 3β5αP does not bind for other reasons. One plausible explanation is that 3β5αP, like cholesterol, has low chemical activity in the membrane and does not achieve sufficiently available concentration to bind in this site (***Lange and Steck, 2016***). This explanation would require that the chemical activity of 3β5αP differs between the inner and outer leaflets of a plasma membrane (presumably due to membrane lipid asymmetry) (***van Meer et al., 2008***; ***Lorent et al., 2020***), since 3β5αP binds to the intrasubunit sites.

The functional analysis of mutations in each of the three NS-binding sites demonstrates that the activating and desensitizing effects of NS result from occupancy of distinct sites. In particular, binding of certain NS (3β5αP, KK148) to α_1 and β_3 intrasubunit sites modulates the open-desensitized equilibrium. Interestingly, lipid binding to intrasubunit pockets in bacterial pLGICs analogous to the α_1 and β_3 intrasubunit sites in $GABA_A$R, also modulates receptor desensitization; docosahexaenoic acid binding to an intrasubunit site in GLIC (***Basak et al., 2017***) and phosphatidylglycerol in ELIC (***Tong et al., 2019***) increase and decrease agonist-induced desensitization, respectively. The

combined results of mutational analyses and binding data demonstrate that the effects of various NS analogues are also a consequence of their efficacy at each of the sites they occupy. For example, KK148 and KK150 occupy the intersubunit site (***Figure 4C***), but do not activate $GABA_AR$ currents (***Figure 1C–D***), and KK150 occupies both intrasubunit sites (***Figure 4B*** and ***Figure 4—figure supplement 1***) but does not desensitize the receptor (***Figure 2B***).

To explain the effects of the 3-substituted NS analogues, we propose a model in which NS-selective binding at three distinct binding sites on the $GABA_AR$ preferentially stabilizes specific states (resting, open, desensitized) of the receptor (***Figure 12***). Orthosteric agonist (GABA or muscimol) binding shifts the equilibrium towards high-affinity states (open and desensitized). 3α5αP allosterically stabilizes the open state through binding to the β_3–α_1 intersubunit and α_1 intrasubunit sites and stabilizes the desensitized state through the β_3 intrasubunit site (***Figure 12A***). In contrast, 3β5αP preferentially stabilizes the desensitized state through binding to both intrasubunit sites (***Figure 12B***). KK148, like 3β5αP, stabilizes the desensitized state by binding to the intrasubunit sites (***Figure 12C***). KK148 also binds to the intersubunit site, presumably with no state-dependence, since it is neither an agonist nor an inverse-agonist (***Figure 1C*** and ***Figure 12C***). KK150, which neither activates nor desensitizes $GABA_ARs$ and is not an inverse agonist, binds to all three sites, again presumably with no-state dependence (***Figure 1D*** and ***Figure 12D***). This model predicts that KK148 should act as a competitive antagonist to PAM-NS at the intersubunit site. This model also predicts that KK150 should be a competitive NS antagonist at all three binding sites. Consistent with this prediction, KK150 antagonizes 3α5αP and KK148 enhancement of [^{3}H]muscimol binding (***Figure 8***).

The site-specific model of NS action (***Figure 12***) has significant implications for the synaptic mechanisms of PAM-NS action. At a synapse, $GABA_ARs$ are transiently exposed to high (mM) concentrations of GABA leading to a channel P_{open} approaching one (***Farrant and Nusser, 2005***; ***Feng and Forman, 2018***). GABA is quickly cleared from the synapse leading to rapid deactivation with minimal desensitization (***Jones and Westbrook, 1995***; ***Overstreet et al., 2000***). In the presence of a PAM-NS, deactivation is slowed, resulting in a prolongation of the IPSC and increased inhibitory current (***Harrison et al., 1987a***; ***Zhu and Vicini, 1997***; ***Harrison et al., 1987b***; ***Chakrabarti et al., 2016***). This effect is largely attributable to stabilization of the open state, presumably by binding to the intersubunit and α_1 intrasubunit binding sites. A second effect has been observed in which the PAM-NS 3α5αP (***Haage and Johansson, 1999***) and 3α5α-THDOC (***Zhu and Vicini, 1997***) prolong the slow component of $GABA_AR$ desensitization and slow recovery from desensitization. This results in increased late channel openings (***Zhu and Vicini, 1997***; ***Jones and Westbrook, 1995***) and IPSC prolongation (***Harrison et al., 1987b***; ***Chakrabarti et al., 2016***). When the frequency of synaptic firing is rapid, the desensitizing effect of NS may also contribute to frequency-dependent reduction in IPSC amplitude (***Zhu and Vicini, 1997***; ***Jones and Westbrook, 1996***). The desensitizing effect of 3α5αP is predominantly mediated by binding at the β_3 intrasubunit site. The balance between stabilization of the open and desensitized channels should be determined by the relative occupancies for the intersubunit site of the active receptor and the β_3 intrasubunit site of the desensitized receptor. Computational docking of 3α5αP to these sites indicates modest differences in affinity between the sites with a rank order affinity of: intersubunit > α_1 intrasubunit > β_3 intrasubunit sites (***Figure 11—source data 1***; ***Chen et al., 2019***). Mutational analysis of the effects of NS on enhancement of [^{3}H]muscimol binding also indicates that 3α5αP has a lower affinity to the β_3 intrasubunit site (***Figure 6B***, ***Table 1***). Thus ,binding to the β_3 intrasubunit site may serve as a negative feedback mechanism preventing excessive PAM-NS effects on synaptic currents.

We have identified specific NS-binding sites on α_1 and β_3 $GABA_ARs$ using photoaffinity labeling, but the structural details of NS interactions with these sites have not yet been elucidated. While several high-resolution structures of αβγ $GABA_ARs$ in a lipidic environment (nano-discs) with bound orthosteric or allosteric ligands have been published (***Laverty et al., 2019***; ***Masiulis et al., 2019***; ***Kim et al., 2020***), there are no available structures of a heteropentameric $GABA_AR$ with a bound NS. There are, however, three X-ray structures of homopentameric, chimeric $GABA_ARs$ crystallized from detergent, all showing NS bound only in the intersubunit site (***Miller et al., 2017***; ***Laverty et al., 2017***; ***Chen et al., 2018***). Since we identified intrasubunit NS-binding sites by photolabeling full-length heteropentameric $GABA_ARs$ in native membranes, it is possible that either the non-natural ECD-TMD junctions or the detergent environment explain why neurosteroid binding to an intrasubunit site was not observed. However, we have also identified an α_1 intrasubunit NS

binding site using a 3α5αP analogue photolabeling reagent in a detergent-solubilized ELIC-α_1 chimeric receptor (**Sugasawa et al., 2019**), indicating that NS can bind to this site in a detergent-solubilized chimeric receptor. It is important to note that there are many reasons why a bound NS (or any other ligand) may not be observed in X-ray or cryo-EM structures and that while these methods provide exquisite detail regarding the structure of ligand binding sites, they should not be regarded as a litmus test for the identification of ligand-binding sites. These reasons include: (1) a protein with steroid bound in the intrasubunit site may not form good crystals or may aggregate, precluding single particle analysis. (2) The conformation(s) observed in the X-ray or cryo-EM structure may not be the conformation to which NS preferentially binds in the intrasubunit site. (3) The ECD-TMD junction is the area of the protein that undergoes the most movement with activation and can be the least well-resolved portion of the transmembrane domains. (4) NS have multiple binding orientations and may be more mobile within the intrasubunit site making them more difficult to resolve. It is also important to consider that our analyses of the functional effects of NS binding were performed using $\alpha_1\beta_3$ $GABA_A$Rs. While the actions of inhibitory and potentiating NS in αβγ or αβδ receptors are qualitatively similar to those observed in αβ receptors, the trimeric receptors may have one less intrasubunit NS-binding site per pentamer, or an intrasubunit with different NS specificity or effect. Additionally, the presence of a γ-subunit has been shown to alter the conformational symmetry of the $GABA_A$R (**Laverty et al., 2019**; **Kim et al., 2020**; **Zhu et al., 2018**) and may influence NS binding to an intrasubunit site or its functional effects.

In summary, this study describes a unique NS pharmacology in which different NS analogues selectively bind to subsets of three sites on the $\alpha_1\beta_3$ $GABA_A$R, with each analogue exhibiting state-dependent binding at a given site. The combination of site-selectivity and state-dependence of binding determines whether a NS analogue is a PAM, a NAM or an antagonist of NS action at the $GABA_A$R. It seems likely that other $GABA_A$R subunit isoforms and heteropentameric subunit combinations will reveal additional NS-binding sites with distinct affinity and state-dependence for various analogues. The identification of potent agonists and antagonists for each of these sites will provide tools for understanding the biological effects of endogenous neurosteroids and potentially for the development of precision neurosteroid therapeutics.

Materials and methods

Construct design

The human α_1 and β_3 $GABA_A$R subunits were subcloned into pcDNA3 for molecular manipulations and cRNA synthesis. Using QuikChange Site-Directed Mutagenesis Kit (Agilent Technologies, Santa Clara, CA), a FLAG tag was first added to the α_1 subunit then an 8xHis tag was added to generate the following His-FLAG tag tandem (QPSLHHHHHHHHDYKDDDDKDEL), inserted between the fourth and fifth residues of the mature peptide. The α_1 and β_3 subunits were then transferred into the pcDNA4/TO and pcDNA5/TO vectors (Thermo Fisher Scientific), respectively, for tetracycline inducible expression. Transient expression was done using the $GABA_A$R subunits rat α_1FLAG (**Ueno et al., 1996**) and human β_3 obtained from Geoffrey White (Neurogen, Branford, CT), each were subcloned into pcDNA3 for molecular manipulations and cRNA synthesis. Point mutations were generated using the QuikChange Site-Directed Mutagenesis Kit (Agilent) and the coding region was fully sequenced prior to use. The cDNAs were linearized with XbaI (NEB Labs, Ipswich, MA), and the cRNAs were generated using T7 mMessage mMachine (Ambion, Austin, TX).

Cell lines

Cell culture was performed as described in previous reports (**Chen et al., 2019**). The tetracycline inducible cell line T-REx-HEK293 (Thermo Fisher Scientific) was cultured under the following conditions: cells were maintained in DMEM/F-12 50/50 medium containing 10% fetal bovine serum (tetracycline-free, Takara, Mountain View, CA), penicillin (100 units/ml), streptomycin (100 g/ml), and blasticidin (2 µg/ml) at 37˚C in a humidified atmosphere containing 5% CO_2. Cells were passaged twice each week, maintaining subconfluent cultures. Stably transfected cells were cultured as above with the addition of hygromycin (50 µg/ml) and zeocin (20 µg/ml). A stable cell line was generated by transfecting T-REx-HEK293 cells with human α_1-8xHis-FLAG pcDNA4/TO and human β_3 pcDNA5/TO, in a 150 mm culture dish, using the Effectene transfection reagent (Qiagen, Germantown, MD).

Two days after transfection, selection of stably transfected cells was performed with hygromycin and zeocin until distinct colonies appeared. Medium was exchanged several times each week to maintain antibiotic selection. Individual clones were selected from the dish and transferred to 24-well plates for expansion of each clone selected. When the cells grew sufficiently, about 50% confluence, they were split into two other plates, one for a surface ELISA against the FLAG epitope and a second for protein assay, to normalize surface expression to cell number. The best eight clones were selected for expansion into 150 mm dishes, followed by [^{3}H]muscimol binding to examine the receptor density. Once the best expressing clone was determined, the highest expressing cells of that clone were selected through fluorescence activated cell sorting. Transient transfections were done in HEK293S GnTI$^-$ cells obtained from ATCC (CRL-3022) using Effectene (Qiagen). The identity of the cell lines has been authenticated using short tandem repeat analysis. Mycoplasma test performed on the cells used for these experiments was negative.

Membrane protein preparation

Stably transfected cells were plated into dishes. After reaching 50% confluence, $GABA_A$ receptors were expressed by inducing cells with 1 µg/ml of doxycycline with the addition of 5 mM sodium butyrate. Cells were harvested 48 to 72 hr after induction. HEK cells, after induction, were grown to 100% confluence, harvested and washed with 10 mM potassium phosphate, 100 mM potassium chloride (pH 7.5) plus protease inhibitors (Sigma-Aldrich, St. Louis, MO) two times. The cells were collected by centrifugation at 1,000 g at 4˚C for 5 min. The cells were homogenized with a glass mortar and a Teflon pestle for ten strokes on ice. The pellet containing the membrane proteins was collected after centrifugation at 20,000 g at 4˚C for 45 min and resuspended in a buffer containing 10 mM potassium phosphate, 100 mM potassium chloride (pH 7.5). The protein concentration was determined with micro-BCA protein assay and membranes were stored at −80˚C.

Photolabeling and purification of $\alpha_1\beta_3$ $GABA_AR$

The syntheses of neurosteroid photolabeling reagents (KK148, KK150, KK200, KK123) are detailed in previous reports (***Jiang et al., 2016***; ***Cheng et al., 2018***). For all the photolabeling experiments, 10–20 mg of HEK cell membrane proteins (about 300 pmol [^{3}H]muscimol binding) were thawed and resuspended in buffer containing 10 mM potassium phosphate, 100 mM potassium chloride (pH 7.5) and 1 mM GABA at a final concentration of 1.25 mg/ml. For the photolabeling competition experiments, 3 µM KK200 or KK123 in the presence of 30 µM competitor (3α5αP, KK148, KK150, and 3β5αP) or the same volume of ethanol was added to the membrane proteins and incubated on ice for 1 hr. The samples were then irradiated in a quartz cuvette for 5 min, by using a photoreactor emitting light at >320 nm. The membrane proteins were then collected by centrifugation at 20,000 g at 4˚C for 45 min. The photolabeled membrane proteins were resuspended in lysis buffer containing 1% *n*-dodecyl-β-D-maltoside (DDM), 0.25% cholesteryl hemisuccinate (CHS), 50 mM Tris (pH 7.5), 150 mM NaCl, 2 mM $CaCl_2$, 5 mM KCl, 5 mM $MgCl_2$, 1 mM EDTA, 10% glycerol at a final concentration of 1 mg/ml. The membrane protein suspension was homogenized using a glass mortar and a Teflon pestle and incubated at 4˚C overnight. The protein lysate was centrifuged at 20,000 g at 4˚C for 45 min and supernatant was incubated with 0.5 ml anti-FLAG agarose (Sigma) at 4˚C for 2 hr. The anti-FLAG agarose was then transferred to an empty column, followed by washing with 20 ml washing buffer (50 mM triethylammonium bicarbonate and 0.05% DDM). The $GABA_ARs$ were eluted with aliquots of 200 µg/ml FLAG tag peptide and 100 µg/ml 3X FLAG (ApexBio) in the washing buffer. The pooled eluates (9 ml) containing $GABA_ARs$ were concentrated to 100 µl using 100 kDa cut-off centrifugal filters.

Tryptic middle-down MS analysis

The purified $\alpha_1\beta_3$ $GABA_AR$ (100 µl) was reduced with 5 mM tris(2-carboxyethyl)phosphine for 1 hr, alkylated with 5 mM *N*-ethylmaleimide (NEM) for 1 hr, and quenched with 5 mM dithiothreitol (DTT) for 15 min. These three steps were done at RT. Samples were then digested with 8 µg of trypsin for 7 days at 4˚C to obtain maximal recovery of TMD peptides. The digestions were terminated by adding formic acid in a final concentration of 1%, followed directly by LC-MS analysis on an Orbitrap Elite mass spectrometer. 20 µl samples were injected into a home-packed PLRP-S (Agilent, Santa Clara, CA) column (10 cm ×75 µm, 300 Å), separated with a 145 min gradient from 10% to 90%

acetonitrile, and introduced to the mass spectrometer at 800 nl/min with a nanospray source. MS acquisition was set as a MS1 Orbitrap scan (resolution of 60,000) followed by top 20 MS2 Orbitrap scans (resolution of 15,000) using data-dependent acquisition, and exclusion of singly charged precursors. Fragmentation was performed using high-energy dissociation with normalized energy of 35%. Analysis of data sets was performed using Xcalibur (Thermo Fisher Scientific) to manually search for TM1, TM2, TM3 or TM4 tryptic peptides with or without neurosteroid photolabeling modifications. Photolabeling efficiency was estimated by generating extracted chromatograms of unlabeled and labeled peptides, determining the area under the curve, and calculating the abundance of labeled peptide/(unlabeled + labeled peptide). Analysis of statistical significance comparing the photolabeling efficiency of KK200 and KK123 for $\alpha_1\beta_3$ $GABA_AR$ was determined using one-way ANOVA with Bonferroni's multiple comparisons test and paired *t*-test, respectively (Prism 6, GraphPad Software, San Diego, CA). MS2 spectra of photolabeled TMD peptides were analyzed by manual assignment of fragment ions with and without photolabeling modification. Fragment ions were accepted based on the presence of a monoisotopic mass within 20 ppm mass accuracy. In addition to manual analysis, PEAKS (Bioinformatics Solutions Inc, Waterloo, ON, Canada) database searches were performed for data sets of photolabeled $\alpha_1\beta_3$ $GABA_AR$. Search parameters were set for a precursor mass accuracy of 20 ppm, fragment ion accuracy of 0.1 Da, up to three missed cleavages on either end of the peptide, false discovery rate of 0.1%, and variable modifications of methionine oxidation, cysteine alkylation with NEM and DTT, and NS analogue photolabeling reagents on any amino acid.

Radioligand-binding assays

[^{3}H]muscimol-binding assays were performed using a previously described method (***Chen et al., 2019***). HEK cell membrane proteins (100 µg/ml final concentration) were incubated with 3 nM [^{3}H]muscimol (30 Ci/mmol; PerkinElmer Life Sciences), neurosteroid (3 nM–30 µM) or etomidate (30 nM–200 µM) in different concentrations and binding buffer (10 mM potassium phosphate, 100 mM potassium chloride, pH 7.5) in a total volume of 1 ml. Assay tubes were incubated for 1 hr on ice in the dark. Nonspecific binding was determined by binding in the presence of 1 mM GABA. Membranes were collected on Whatman/GF-C glass filter papers using a Brandel cell harvester (Gaithersburg, MD). To perform [^{3}H]muscimol binding isotherms, 100 µg/ml aliquots of membrane protein were incubated with 0.3 nM–1 µM [^{3}H]muscimol for 1 hr on ice in the dark. The specific activity for [^{3}H]muscimol concentrations from 30 nM to 1 µM was reduced to 2 Ci/mmol by dilution with nonradioactive muscimol. The membranes were collected on Whatman/GF-B glass filter papers using a vacuum manifold. Raw concentration-dependent total and nonspecific binding and calculated specific binding data from a representative experiment (WT receptors, no NS) are shown in ***Figure 7—figure supplement 1***. For [^{3}H]muscimol-binding experiments examining competitive interactions between neurosteroids, the combined neurosteroids (0.3 µM 3α5αP or 3 µM KK148 ±30 µM KK150) or the same volume of dimethyl sulfoxide (DMSO) were added to the membranes which were then incubated with 3 nM [^{3}H]muscimol on ice for 1 hr. Time courses of neurosteroid [^{3}H]muscimol binding enhancement were examined by adding 10 µM of neurosteroids (3α5αP, 3β5αP) to membranes that had been fully equilibrated with 3 nM [^{3}H]muscimol for 1 hr on ice; binding was then measured as a function of time at 1, 3, 10, 30, 60 min. The membranes were collected on Whatman/GF-B glass filter papers using a vacuum manifold. Radioactivity bound to the filters was measured by liquid scintillation spectrometry using Bio-Safe II (Research Products International, Mount Prospect, IL).

Radioligand binding to intact cells

HEK cells were harvested by gently washing dishes with buffer containing 10 mM sodium phosphate (pH 7.5), 150 mM sodium chloride twice. The cells were collected by centrifugation at 500 g at 4˚C for 5 min, and resuspended in isotonic (10 mM sodium phosphate, 150 mM sodium chloride, pH 7.5) or hypotonic (10 mM sodium phosphate, pH 7.5) buffer to prepare two different conditions for radioligand binding to intact cells [isotonic buffer for cell surface receptors; hypotonic buffer for total receptors (cell surface receptors + intracellular receptors)]. The cells were incubated on ice for 2 hr, after which the sodium chloride concentration was adjusted to be isotonic before the radioligand binding procedure. HEK cells were aliquoted to assay tubes (20 samples/150 mm dish) in a total volume of 1 ml, and incubated with 3 nM [^{3}H]muscimol ±10 µM KK148 for 1 hr on ice in the dark.

Nonspecific binding was determined by binding in the presence of 1 mM GABA. The membranes were collected on Whatman/GF-B glass filter papers using a vacuum manifold. Radioactivity bound to the filters was measured by liquid scintillation spectrometry using Bio-Safe II.

Receptor expression in *Xenopus laevis* oocytes and electrophysiological recordings

The wild-type and mutant $\alpha_1\beta_3$ $GABA_AR$ were expressed in oocytes from the African clawed frog (*Xenopus laevis*). Frogs were purchased from Xenopus 1 (Dexter, MI), and housed and cared for in a Washington University Animal Care Facility under the supervision of the Washington University Division of Comparative Medicine. Harvesting of oocytes was conducted under the Guide for the Care and Use of Laboratory Animals as adopted and promulgated by the National Institutes of Health. The animal protocol (No. 20180191) was approved by the Animal Studies Committee of Washington University in St. Louis. The oocytes were injected with a total of 12 ng cRNA. The ratio of cRNAs was 5:1 ratio (α_1:β_3) to minimize the expression of β_3 homomeric receptors. Following injection, the oocytes were incubated in ND96 (96 mM NaCl, 2 mM KCl, 1.8 mM $CaCl_2$, 1 mM $MgCl_2$, 5 mM HEPES; pH 7.4) with supplements (2.5 mM Na pyruvate, 100 U/ml penicillin, 100 µg/ml streptomycin and 50 µg/ml gentamycin) at 16˚C for 2 days prior to conducting electrophysiological recordings. The electrophysiological recordings were conducted at room temperature using standard two-electrode voltage clamp. The oocytes were clamped at −60 mV. The chamber (RC-1Z, Warner Instruments, Hamden, CT) was perfused with ND96 at 5–8 ml/min. Solutions were gravity-applied from 30 ml glass syringes with glass luer slips via Teflon tubing. The current responses were amplified with an OC-725C amplifier (Warner Instruments, Hamden, CT), digitized with a Digidata 1200 series digitizer (Molecular Devices), and stored using pClamp (Molecular Devices). Current traces were analyzed with Clampfit (Molecular Devices). Activation by steroids (***Figure 1***) was tested by coapplying a steroid with 0.3 µM GABA (P_{open} = 0.05–0.1). The desensitizing effects of steroids (***Figures 9–10***) were tested by coapplying a steroid with 1 mM (saturating) GABA, alone or in the presence of PB, during the steady-state phase of the current response. The combination of GABA and PB was used to activate some combinations of mutations to maintain a consistent, high peak open probability (0.55–0.95). In control experiments in WT $\alpha_1\beta_3$ $GABA_ARs$, pentobarbital had no effect on 3β5αP inhibition of steady-state current (data not shown). The stock solution of GABA was made in ND96 at 500 mM, stored in aliquots at −20˚C, and diluted on the day of experiment. The stock solution of muscimol was made at 20 mM in ND96 and stored at 4˚C. The steroids were dissolved in DMSO at 10–20 mM and stored at room temperature.

Electrophysiological data analysis and simulations

The raw amplitudes of the current traces were converted to units of open probability through comparison to the peak response to 1 mM GABA + 50 µM propofol, that was considered to have a peak P_{open} indistinguishable from 1 (***Chen et al., 2019***). The level of constitutive activity in the absence of any applied agonist was considered negligible and not included in this calculation. The converted current traces were analyzed in the framework of the three-state Resting-Open-Desensitized activation model (***Germann et al., 2019a***; ***Germann et al., 2019b***). The model enables analysis and prediction of peak responses using four parameters that characterize the extent of constitutive activity (termed L; L = Resting/Open), affinity of the resting receptor to agonist (K_C), affinity of the open receptor to agonist (K_O), and the number of agonist binding sites (N). Analysis and prediction of steady-state responses requires an additional parameter, termed Q, that describes the equilibrium between open and desensitized receptors (Q = Open/Desensitized).

The P_{open} of the peak response is expressed as:

$$P_{open,peak} = \frac{1}{1 + L\Gamma}$$

and the P_{open} of the steady-state response as:

$$\mathrm{P}_{\mathrm{open,steady-state}} = \frac{1}{1 + \frac{1}{\mathrm{Q}} + \mathrm{L}\Gamma}$$

where

$$\Gamma = \left[\frac{(1+[X]/K_C)}{(1+[X]/K_O)}\right]^N$$

[X]is the concentration of agonist present, and other terms are as described above. In practice, the value of LΓ was calculated using the experimentally determined P_{open} of the peak response, and then used as a fixed value in estimating Q from $P_{open,steady\text{-}state}$.

The $P_{desensitized}$ was calculated using:

$$P_{desensitized} = \frac{1}{1+Q+QL\Gamma}$$

The effect of 3β5αP on 1 mM GABA-elicited steady-state current was expressed through a change in the value of Q. The modified Q (termed Q*) was then used to predict changes in P_{open} and $P_{desensitized}$ at low [GABA]. Calculated probabilities (e.g. P_{open}, $P_{desentitized}$) are reported as mean ± SD.

Docking simulations

A model of the $\alpha_1\beta_3$ $GABA_AR$ was developed using the crystal structure of the human β_3 homopentamer (PDB ID: 4COF) as a structural template (***Miller and Aricescu, 2014***). In this structure, the cytoplasmic loop was replaced with the sequence SQPARAA (***Jansen et al., 2008***). The pentamer subunits were organized as A α_1, B β_3, C α_1, D β_3, E β_3. The α_1 sequence was aligned to the β_3 sequence using the program MUSCLE (***Edgar, 2004***). The pentameric alignment was then used as input for the program Modeller (***Sali and Blundell, 1993***), using 4COF as the template; a total of 25 models were generated. The best model as evaluated by the DOPE score (***Shen and Sali, 2006***) was then submitted to the H++ server (http://biophysics.cs.vt.edu) to determine charges and optimize hydrogen bonding. The optimized structure was then submitted to the PPM server (https://opm.phar.umich.edu/ppm_server) for orientation into a lipid membrane. The correctly oriented receptor was then submitted to the CHARMM-GUI Membrane Builder server (http://www.charmm-gui.org) to build the fully solvated, membrane bound system oriented into a 1-palmitoyl-2-oleoyl-sn-glycero-3-phosphatidylcholine (POPC) bilayer. The system was fully solvated with 40715 TIP3 water molecules and ionic strength set to 0.15 M KCl. The NAMD input files produced by CHARMM-GUI (***Lee et al., 2016***) use a seven-step process of gradually loosening constraints in the simulation prior to production runs. A 100 ns molecular dynamics trajectory was then obtained using the CHARMM36 force field and NAMD (***Lee et al., 2016***). The resulting trajectory was then processed using the utility mdtraj (***McGibbon et al., 2015***), to extract a snapshot of the receptor at each nanosecond of time frame. These structures were then mutually aligned by fitting the alpha carbons, providing a set of 100 mutually aligned structures used for docking studies. The docking was performed using AutoDock Vina (***Trott and Olson, 2010***) on each of the 100 snapshots in order to capture receptor flexibility. 3α5αP and 3β5αP were prepared by converting the sdf file from PubChem into a PDB file using Open Babel (***O'Boyle et al., 2011***), and Gasteiger charges and free torsion angles were determined by AutoDock Tools. Docking grid boxes were built for the β_3–α_1 intersubunit, and the α_1 and β_3 intrasubunit sites with dimensions of 15 × 15 × 15 Ångströms encompassing each binding pocket. Docking was limited to an energy range of 3 kcal from the best docking pose and was limited to a total of 20 unique poses. The docking results for a given site could result in a maximum of 2000 unique poses (20 poses × 100 receptor structures); these were then clustered geometrically using the program DIVCF (***Meslamani et al., 2009***). The resulting clusters were ranked by Vina score and cluster size, and then visually analyzed. A comparison of proposed NS-binding sites between the modeled $\alpha_1\beta_3$ $GABA_AR$ TMD and the experimentally determined $\alpha_1\beta_3\gamma_2$ cryo-EM structure PDB ID: 6I53 (***Laverty et al., 2019***) was performed. The two structures were read into UCSF Chimera and mutually aligned using MatchMaker (***Meng et al., 2006***). Using the same Vina docking configuration files discussed above, 3α5αP and 3β5αP were then docked into the respective sites of the $\alpha_1\beta_3\gamma_2$ cryo-EM structure. The results are shown in ***Figure 11*** and ***Figure 11—source data 1***; there was very little difference in the results between the modeled $\alpha_1\beta_3$ and the $\alpha_1\beta_3\gamma_2$ cryo-EM structure.

Acknowledgements

The authors thank Drs. Charles F Zorumski, Steven Mennerick and Joseph Henry Steinbach for insightful advice and valuable suggestions.

Additional information

Funding

Funder	Grant reference number	Author
National Institutes of Health	2R01GM108799-05	Alex S Evers Douglas F Covey
National Institutes of Health	5K08GM126336-03	Wayland WL Cheng
National Institutes of Health	5R01GM108580-06	Gustav Akk
Taylor Family Institute for Innovative Psychiatric Research		Zi-Wei Chen David E Reichert Douglas F Covey Gustav Akk Alex S Evers

The funders had no role in study design, data collection and interpretation, or the decision to submit the work for publication.

Author contributions

Yusuke Sugasawa, Data curation, Formal analysis, Investigation, Visualization, Writing - original draft, Project administration; Wayland WL Cheng, Methodology, Writing - review and editing; John R Bracamontes, Kathiresan Krishnan, Investigation, Methodology; Zi-Wei Chen, Investigation, Methodology, Writing - review and editing; Lei Wang, Data curation; Allison L Germann, Spencer R Pierce, Thomas C Senneff, Data curation, Investigation; David E Reichert, Data curation, Formal analysis, Investigation, Methodology, Writing - review and editing; Douglas F Covey, Resources, Supervision, Funding acquisition, Validation, Investigation, Methodology, Writing - review and editing; Gustav Akk, Conceptualization, Data curation, Formal analysis, Supervision, Funding acquisition, Validation, Investigation, Methodology, Writing - review and editing; Alex S Evers, Conceptualization, Resources, Software, Supervision, Funding acquisition, Validation, Visualization, Methodology, Writing - original draft, Project administration

Author ORCIDs

Yusuke Sugasawa https://orcid.org/0000-0003-1607-0460
Wayland WL Cheng http://orcid.org/0000-0002-9529-9820
Zi-Wei Chen http://orcid.org/0000-0001-8601-2210
Alex S Evers https://orcid.org/0000-0002-0342-0575

Decision letter and Author response

Decision letter https://doi.org/10.7554/eLife.55331.sa1
Author response https://doi.org/10.7554/eLife.55331.sa2

Additional files

Supplementary files

- Transparent reporting form

Data availability

All data generated or analysed during this study are included in the manuscript and supporting files.

References

Abramian AM, Comenencia-Ortiz E, Modgil A, Vien TN, Nakamura Y, Moore YE, Maguire JL, Terunuma M, Davies PA, Moss SJ. 2014. Neurosteroids promote phosphorylation and membrane insertion of extrasynaptic GABAA receptors. *PNAS* **111**:7132–7137. DOI: https://doi.org/10.1073/pnas.1403285111, PMID: 24778259

Akk G, Bracamontes J, Steinbach JH. 2001. Pregnenolone sulfate block of $_{GABA(A)}$ receptors: mechanism and involvement of a residue in the M2 region of the alpha subunit. *The Journal of Physiology* **532**:673–684. DOI: https://doi.org/10.1111/j.1469-7793.2001.0673e.x, PMID: 11313438

Akk G, Bracamontes JR, Covey DF, Evers A, Dao T, Steinbach JH. 2004. Neuroactive steroids have multiple actions to potentiate GAB_{AA} receptors. *The Journal of Physiology* **558**:59–74. DOI: https://doi.org/10.1113/jphysiol.2004.066571, PMID: 15146041

Akk G, Covey DF, Evers AS, Steinbach JH, Zorumski CF, Mennerick S. 2007. Mechanisms of neurosteroid interactions with GABA(A) receptors. *Pharmacology & Therapeutics* **116**:35–57. DOI: https://doi.org/10.1016/j.pharmthera.2007.03.004, PMID: 17524487

Akk G, Li P, Bracamontes J, Reichert DE, Covey DF, Steinbach JH. 2008. Mutations of the GABA-A receptor alpha1 subunit M1 domain reveal unexpected complexity for modulation by neuroactive steroids. *Molecular Pharmacology* **74**:614–627. DOI: https://doi.org/10.1124/mol.108.048520, PMID: 18544665

Akk G, Covey DF, Evers AS, Mennerick S, Zorumski CF, Steinbach JH. 2010. Kinetic and structural determinants for GABA-A receptor potentiation by neuroactive steroids. *Current Neuropharmacology* **8**:18–25. DOI: https://doi.org/10.2174/157015910790909458, PMID: 20808543

Akk G, Germann AL, Sugasawa Y, Pierce SR, Evers AS, Steinbach JH. 2020. Enhancement of muscimol binding and gating by allosteric modulators of the GAB_{AA} Receptor: Relating Occupancy to State Functions. *Molecular Pharmacology* **98**:303–313. DOI: https://doi.org/10.1124/molpharm.120.000066, PMID: 32873746

Basak S, Schmandt N, Gicheru Y, Chakrapani S. 2017. Crystal structure and dynamics of a lipid-induced potential desensitized-state of a pentameric ligand-gated channel. *eLife* **6**:e23886. DOI: https://doi.org/10.7554/eLife.23886, PMID: 28262093

Belelli D, Lambert JJ. 2005. Neurosteroids: endogenous regulators of the GABA(A) receptor. *Nature Reviews Neuroscience* **6**:565–575. DOI: https://doi.org/10.1038/nrn1703, PMID: 15959466

Bianchi MT, Macdonald RL. 2003. Neurosteroids shift partial agonist activation of $_{GABA(A)}$ receptor channels from low- to high-efficacy gating patterns. *The Journal of Neuroscience* **23**:10934–10943. DOI: https://doi.org/10.1523/JNEUROSCI.23-34-10934.2003, PMID: 14645489

Bracamontes JR, Steinbach JH. 2009. Steroid interaction with a single potentiating site is sufficient to modulate GABA-A receptor function. *Molecular Pharmacology* **75**:973–981. DOI: https://doi.org/10.1124/mol.108.053629, PMID: 19176850

Budelier MM, Cheng WWL, Bergdoll L, Chen ZW, Janetka JW, Abramson J, Krishnan K, Mydock-McGrane L, Covey DF, Whitelegge JP, Evers AS. 2017. Photoaffinity labeling with cholesterol analogues precisely maps a cholesterol-binding site in voltage-dependent anion channel-1. *Journal of Biological Chemistry* **292**:9294–9304. DOI: https://doi.org/10.1074/jbc.M116.773069, PMID: 28396346

Budelier MM, Cheng WWL, Chen Z-W, Bracamontes JR, Sugasawa Y, Krishnan K, Mydock-McGrane L, Covey DF, Evers AS. 2019. Common binding sites for cholesterol and neurosteroids on a pentameric ligand-gated ion channel. *Biochimica Et Biophysica Acta (BBA) - Molecular and Cell Biology of Lipids* **1864**:128–136. DOI: https://doi.org/10.1016/j.bbalip.2018.11.005

Bylund DB, Deupree JD, Toews ML. 2004. Radioligand-binding methods for membrane preparations and intact cells. *Methods in Molecular Biology* **259**:1–28. DOI: https://doi.org/10.1385/1-59259-754-8:001, PMID: 15250483

Bylund DB, Toews ML. 1993. Radioligand binding methods: practical guide and tips. *American Journal of Physiology-Lung Cellular and Molecular Physiology* **265**:L421–L429. DOI: https://doi.org/10.1152/ajplung.1993.265.5.L421

Chakrabarti S, Qian M, Krishnan K, Covey DF, Mennerick S, Akk G. 2016. Comparison of steroid modulation of spontaneous inhibitory postsynaptic currents in cultured hippocampal neurons and Steady-State Single-Channel currents from heterologously expressed α1β2γ2l $_{GABA(A)}$ Receptors. *Molecular Pharmacology* **89**:399–406. DOI: https://doi.org/10.1124/mol.115.102202, PMID: 26769414

Chang Y, Ghansah E, Chen Y, Ye J, Weiss DS, Chang Y. 2002. Desensitization mechanism of GABA receptors revealed by single oocyte binding and receptor function. *The Journal of Neuroscience* **22**:7982–7990. DOI: https://doi.org/10.1523/JNEUROSCI.22-18-07982.2002, PMID: 12223551

Chen Q, Wells MM, Arjunan P, Tillman TS, Cohen AE, Xu Y, Tang P. 2018. Structural basis of neurosteroid anesthetic action on GAB_{AA} receptors. *Nature Communications* **9**:3972. DOI: https://doi.org/10.1038/s41467-018-06361-4, PMID: 30266951

Chen ZW, Bracamontes JR, Budelier MM, Germann AL, Shin DJ, Kathiresan K, Qian MX, Manion B, Cheng WWL, Reichert DE, Akk G, Covey DF, Evers AS. 2019. Multiple functional neurosteroid binding sites on GABAA receptors. *PLOS Biology* **17**:e3000157. DOI: https://doi.org/10.1371/journal.pbio.3000157, PMID: 30845142

Cheng WWL, Chen ZW, Bracamontes JR, Budelier MM, Krishnan K, Shin DJ, Wang C, Jiang X, Covey DF, Akk G, Evers AS. 2018. Mapping two neurosteroid-modulatory sites in the prototypic pentameric ligand-gated ion channel GLIC. *Journal of Biological Chemistry* **293**:3013–3027. DOI: https://doi.org/10.1074/jbc.RA117.000359, PMID: 29301936

Comenencia-Ortiz E, Moss SJ, Davies PA. 2014. Phosphorylation of GABAA receptors influences receptor trafficking and neurosteroid actions. *Psychopharmacology* **231**:3453–3465. DOI: https://doi.org/10.1007/s00213-014-3617-z, PMID: 24847959

Das J. 2011. Aliphatic diazirines as photoaffinity probes for proteins: recent developments. *Chemical Reviews* **111**:4405–4417. DOI: https://doi.org/10.1021/cr1002722, PMID: 21466226

Dostalova Z, Zhou X, Liu A, Zhang X, Zhang Y, Desai R, Forman SA, Miller KW. 2014. Human α1β3γ2l gamma-aminobutyric acid type A receptors: high-level production and purification in a functional state. *Protein Science* **23**:157–166. DOI: https://doi.org/10.1002/pro.2401, PMID: 24288268

Eaton M, Germann A, Arora R, Cao L, Gao X, Shin D, Wu A, Chiara D, Cohen J, Henry Steinbach J, Evers A, Akk G. 2016. Multiple Non-Equivalent interfaces mediate direct activation of GABAA receptors by propofol. *Current Neuropharmacology* **14**:772–780. DOI: https://doi.org/10.2174/1570159X14666160202121319

Edgar RC. 2004. MUSCLE: a multiple sequence alignment method with reduced time and space complexity. *BMC Bioinformatics* **5**:113. DOI: https://doi.org/10.1186/1471-2105-5-113, PMID: 15318951

Evers AS, Chen ZW, Manion BD, Han M, Jiang X, Darbandi-Tonkabon R, Kable T, Bracamontes J, Zorumski CF, Mennerick S, Steinbach JH, Covey DF. 2010. A synthetic 18-norsteroid distinguishes between two neuroactive steroid binding sites on GABAA receptors. *Journal of Pharmacology and Experimental Therapeutics* **333**:404–413. DOI: https://doi.org/10.1124/jpet.109.164079, PMID: 20124410

Farrant M, Nusser Z. 2005. Variations on an inhibitory theme: phasic and tonic activation of GABAA receptors. *Nature Reviews Neuroscience* **6**:215–229. DOI: https://doi.org/10.1038/nrn1625

Feng HJ, Forman SA. 2018. Comparison of αβδ and αβγ GAB_{AA} receptors: Allosteric modulation and identification of subunit arrangement by site-selective general anesthetics. *Pharmacological Research* **133**:289–300. DOI: https://doi.org/10.1016/j.phrs.2017.12.031, PMID: 29294355

Germann AL, Pierce SR, Burbridge AB, Steinbach JH, Akk G. 2019a. Steady-State activation and modulation of the concatemeric alpha 1 beta 2 gamma 2L GABA(A) Receptor. *Molecular Pharmacology* **96**:320–329. DOI: https://doi.org/10.1124/mol.119.116913

Germann AL, Pierce SR, Senneff TC, Burbridge AB, Steinbach JH, Akk G. 2019b. Steady-state activation and modulation of the synaptic-type α1β2γ2l GAB_{AA} receptor by combinations of physiological and clinical ligands. *Physiological Reports* **7**:e14230. DOI: https://doi.org/10.14814/phy2.14230, PMID: 31549483

Gielen M, Corringer PJ. 2018. The dual-gate model for pentameric ligand-gated ion channels activation and desensitization. *The Journal of Physiology* **596**:1873–1902. DOI: https://doi.org/10.1113/JP275100, PMID: 29484660

Grobin AC, Gizerian S, Lieberman JA, Morrow AL. 2006. Perinatal allopregnanolone influences prefrontal cortex structure, connectivity and behavior in adult rats. *Neuroscience* **138**:809–819. DOI: https://doi.org/10.1016/j.neuroscience.2005.12.026, PMID: 16457952

Gunduz-Bruce H, Silber C, Kaul I, Rothschild AJ, Riesenberg R, Sankoh AJ, Li H, Lasser R, Zorumski CF, Rubinow DR, Paul SM, Jonas J, Doherty JJ, Kanes SJ. 2019. Trial of SAGE-217 in patients with major depressive disorder. *New England Journal of Medicine* **381**:903–911. DOI: https://doi.org/10.1056/NEJMoa1815981, PMID: 31483961

Haage D, Johansson S. 1999. Neurosteroid modulation of synaptic and GABA-evoked currents in neurons from the rat medial preoptic nucleus. *Journal of Neurophysiology* **82**:143–151. DOI: https://doi.org/10.1152/jn.1999.82.1.143, PMID: 10400943

Harrison NL, Majewska MD, Harrington JW, Barker JL. 1987a. Structure-activity relationships for steroid interaction with the gamma-aminobutyric acidA receptor complex. *The Journal of Pharmacology and Experimental Therapeutics* **241**:346–353. PMID: 3033209

Harrison NL, Vicini S, Barker JL. 1987b. A steroid anesthetic prolongs inhibitory postsynaptic currents in cultured rat hippocampal neurons. *The Journal of Neuroscience* **7**:604–609. DOI: https://doi.org/10.1523/JNEUROSCI.07-02-00604.1987, PMID: 3819824

Harrison NL, Simmonds MA. 1984. Modulation of the GABA receptor complex by a steroid anaesthetic. *Brain Research* **323**:287–292. DOI: https://doi.org/10.1016/0006-8993(84)90299-3

Hosie AM, Wilkins ME, da Silva HM, Smart TG. 2006. Endogenous neurosteroids regulate GABAA receptors through two discrete transmembrane sites. *Nature* **444**:486–489. DOI: https://doi.org/10.1038/nature05324, PMID: 17108970

Hosie AM, Clarke L, da Silva H, Smart TG. 2009. Conserved site for neurosteroid modulation of GABA A receptors. *Neuropharmacology* **56**:149–154. DOI: https://doi.org/10.1016/j.neuropharm.2008.07.050, PMID: 18762201

Jansen M, Bali M, Akabas MH. 2008. Modular design of Cys-loop ligand-gated ion channels: functional 5-HT3 and GABA rho1 receptors lacking the large cytoplasmic M3M4 loop. *Journal of General Physiology* **131**:137–146. DOI: https://doi.org/10.1085/jgp.200709896, PMID: 18227272

Jayakar SS, Zhou X, Chiara DC, Jarava-Barrera C, Savechenkov PY, Bruzik KS, Tortosa M, Miller KW, Cohen JB. 2019. Identifying drugs that bind selectively to intersubunit general anesthetic sites in the alpha1beta3gamma2 GABAAR transmembrane domain. *Molecular Pharmacology* **95**:615–628. DOI: https://doi.org/10.1124/mol.118.114975

Jayakar SS, Chiara DC, Zhou X, Wu B, Bruzik KS, Miller KW, Cohen JB. 2020. Photoaffinity labeling identifies an intersubunit steroid-binding site in heteromeric GAB_A type $_A$ (GAB_{AA}) receptors . *Journal of Biological Chemistry* **295**:11495–11512. DOI: https://doi.org/10.1074/jbc.RA120.013452

Jiang X, Shu HJ, Krishnan K, Qian M, Taylor AA, Covey DF, Zorumski CF, Mennerick S. 2016. A clickable neurosteroid photolabel reveals selective golgi compartmentalization with preferential impact on proximal

inhibition. *Neuropharmacology* **108**:193–206. DOI: https://doi.org/10.1016/j.neuropharm.2016.04.031, PMID: 27114255

Jones MV, Westbrook GL. 1995. Desensitized states prolong GABAA channel responses to brief agonist pulses. *Neuron* **15**:181–191. DOI: https://doi.org/10.1016/0896-6273(95)90075-6, PMID: 7542462

Jones MV, Westbrook GL. 1996. The impact of receptor desensitization on fast synaptic transmission. *Trends in Neurosciences* **19**:96–101. DOI: https://doi.org/10.1016/S0166-2236(96)80037-3, PMID: 9054063

Kharasch ED, Hollmann MW. 2015. Steroid anesthesia revisited. *Anesthesia & Analgesia* **120**:983–984. DOI: https://doi.org/10.1213/ANE.0000000000000667

Kim JJ, Gharpure A, Teng J, Zhuang Y, Howard RJ, Zhu S, Noviello CM, Walsh RM, Lindahl E, Hibbs RE. 2020. Shared structural mechanisms of general anaesthetics and benzodiazepines. *Nature* **585**:303–308. DOI: https://doi.org/10.1038/s41586-020-2654-5, PMID: 32879488

Lange Y, Steck TL. 2016. Active membrane cholesterol as a physiological effector. *Chemistry and Physics of Lipids* **199**:74–93. DOI: https://doi.org/10.1016/j.chemphyslip.2016.02.003, PMID: 26874289

Laverty D, Thomas P, Field M, Andersen OJ, Gold MG, Biggin PC, Gielen M, Smart TG. 2017. Crystal structures of a GAB_{AA}-receptor chimera reveal new endogenous neurosteroid-binding sites. *Nature Structural & Molecular Biology* **24**:977–985. DOI: https://doi.org/10.1038/nsmb.3477, PMID: 28967882

Laverty D, Desai R, Uchański T, Masiulis S, Stec WJ, Malinauskas T, Zivanov J, Pardon E, Steyaert J, Miller KW, Aricescu AR. 2019. Cryo-EM structure of the human $\alpha1\beta3\gamma2$ GAB_{AA} receptor in a lipid bilayer. *Nature* **565**:516–520. DOI: https://doi.org/10.1038/s41586-018-0833-4, PMID: 30602789

Lee J, Cheng X, Swails JM, Yeom MS, Eastman PK, Lemkul JA, Wei S, Buckner J, Jeong JC, Qi Y, Jo S, Pande VS, Case DA, Brooks CL, MacKerell AD, Klauda JB, Im W. 2016. CHARMM-GUI input generator for NAMD, GROMACS, AMBER, OpenMM, and CHARMM/OpenMM simulations using the CHARMM36 additive force field. *Journal of Chemical Theory and Computation* **12**:405–413. DOI: https://doi.org/10.1021/acs.jctc.5b00935, PMID: 26631602

Li GD, Chiara DC, Sawyer GW, Husain SS, Olsen RW, Cohen JB. 2006. Identification of a GABAA receptor anesthetic binding site at subunit interfaces by photolabeling with an etomidate analog. *The Journal of Neuroscience* **26**:11599–11605. DOI: https://doi.org/10.1523/JNEUROSCI.3467-06.2006, PMID: 17093081

Li P, Shu HJ, Wang C, Mennerick S, Zorumski CF, Covey DF, Steinbach JH, Akk G. 2007. Neurosteroid migration to intracellular compartments reduces steroid concentration in the membrane and diminishes GABA-A receptor potentiation. *The Journal of Physiology* **584**:789–800. DOI: https://doi.org/10.1113/jphysiol.2007.142794, PMID: 17761771

Lorent JH, Levental KR, Ganesan L, Rivera-Longsworth G, Sezgin E, Doktorova M, Lyman E, Levental I. 2020. Plasma membranes are asymmetric in lipid Unsaturation, packing and protein shape. *Nature Chemical Biology* **16**:644–652. DOI: https://doi.org/10.1038/s41589-020-0529-6, PMID: 32367017

Lundgren P, Strömberg J, Bäckström T, Wang M. 2003. Allopregnanolone-stimulated GABA-mediated chloride ion flux is inhibited by 3beta-hydroxy-5alpha-pregnan-20-one (isoallopregnanolone). *Brain Research* **982**:45–53. DOI: https://doi.org/10.1016/S0006-8993(03)02939-1, PMID: 12915239

Masiulis S, Desai R, Uchański T, Serna Martin I, Laverty D, Karia D, Malinauskas T, Zivanov J, Pardon E, Kotecha A, Steyaert J, Miller KW, Aricescu AR. 2019. GAB_{AA} receptor signalling mechanisms revealed by structural pharmacology. *Nature* **565**:454–459. DOI: https://doi.org/10.1038/s41586-018-0832-5, PMID: 30602790

McGibbon RT, Beauchamp KA, Harrigan MP, Klein C, Swails JM, Hernández CX, Schwantes CR, Wang LP, Lane TJ, Pande VS. 2015. MDTraj: a modern open library for the analysis of molecular dynamics trajectories. *Biophysical Journal* **109**:1528–1532. DOI: https://doi.org/10.1016/j.bpj.2015.08.015, PMID: 26488642

Meng EC, Pettersen EF, Couch GS, Huang CC, Ferrin TE. 2006. Tools for integrated sequence-structure analysis with UCSF chimera. *BMC Bioinformatics* **7**:339. DOI: https://doi.org/10.1186/1471-2105-7-339, PMID: 16836757

Meslamani JE, André F, Petitjean M. 2009. Assessing the geometric diversity of cytochrome P450 ligand conformers by hierarchical clustering with a stop criterion. *Journal of Chemical Information and Modeling* **49**:330–337. DOI: https://doi.org/10.1021/ci800275k, PMID: 19434834

Miller PS, Scott S, Masiulis S, De Colibus L, Pardon E, Steyaert J, Aricescu AR. 2017. Structural basis for GAB_{AA} receptor potentiation by neurosteroids. *Nature Structural & Molecular Biology* **24**:986–992. DOI: https://doi.org/10.1038/nsmb.3484, PMID: 28991263

Miller PS, Aricescu AR. 2014. Crystal structure of a human GABAA receptor. *Nature* **512**:270–275. DOI: https://doi.org/10.1038/nature13293, PMID: 24909990

Mitchell EA, Herd MB, Gunn BG, Lambert JJ, Belelli D. 2008. Neurosteroid modulation of GABAA receptors: molecular determinants and significance in health and disease. *Neurochemistry International* **52**:588–595. DOI: https://doi.org/10.1016/j.neuint.2007.10.007, PMID: 18055067

O'Boyle NM, Banck M, James CA, Morley C, Vandermeersch T, Hutchison GR. 2011. Open babel: an open chemical toolbox. *Journal of Cheminformatics* **3**:33. DOI: https://doi.org/10.1186/1758-2946-3-33, PMID: 21982300

Olsen RW. 2018. GAB_{AA} receptor: Positive and negative allosteric modulators. *Neuropharmacology* **136**:10–22. DOI: https://doi.org/10.1016/j.neuropharm.2018.01.036, PMID: 29407219

Olsen RW, Sieghart W. 2008. International union of pharmacology LXX subtypes of gamma-aminobutyric acid(A) receptors: classification on the basis of subunit composition, pharmacology, and function update. *Pharmacological Reviews* **60**:243–260. DOI: https://doi.org/10.1124/pr.108.00505, PMID: 18790874

Overstreet LS, Jones MV, Westbrook GL. 2000. Slow desensitization regulates the availability of synaptic GABA (A) receptors. *The Journal of Neuroscience* **20**:7914–7921. DOI: https://doi.org/10.1523/JNEUROSCI.20-21-07914.2000, PMID: 11050111

Park-Chung M, Malayev A, Purdy RH, Gibbs TT, Farb DH. 1999. Sulfated and unsulfated steroids modulate gamma-aminobutyric acidA receptor function through distinct sites. *Brain Research* **830**:72–87. DOI: https://doi.org/10.1016/S0006-8993(99)01381-5, PMID: 10350561

Reddy DS, Estes WA. 2016. Clinical potential of neurosteroids for CNS disorders. *Trends in Pharmacological Sciences* **37**:543–561. DOI: https://doi.org/10.1016/j.tips.2016.04.003, PMID: 27156439

Represa A, Ben-Ari Y. 2005. Trophic actions of GABA on neuronal development. *Trends in Neurosciences* **28**: 278–283. DOI: https://doi.org/10.1016/j.tins.2005.03.010, PMID: 15927682

Sali A, Blundell TL. 1993. Comparative protein modelling by satisfaction of spatial restraints. *Journal of Molecular Biology* **234**:779–815. DOI: https://doi.org/10.1006/jmbi.1993.1626, PMID: 8254673

Seljeset S, Bright DP, Thomas P, Smart TG. 2018. Probing GAB_{AA} receptors with inhibitory neurosteroids. *Neuropharmacology* **136**:23–36. DOI: https://doi.org/10.1016/j.neuropharm.2018.02.008, PMID: 29447845

Shen W, Mennerick S, Covey DF, Zorumski CF. 2000. Pregnenolone sulfate modulates inhibitory synaptic transmission by enhancing $_{GABA(A)}$ receptor desensitization. *The Journal of Neuroscience* **20**:3571–3579. DOI: https://doi.org/10.1523/JNEUROSCI.20-10-03571.2000, PMID: 10804198

Shen MY, Sali A. 2006. Statistical potential for assessment and prediction of protein structures. *Protein Science* **15**:2507–2524. DOI: https://doi.org/10.1110/ps.062416606, PMID: 17075131

Sieghart W. 2015. Allosteric modulation of GABAA receptors via multiple drug-binding sites. *Advances in Pharmacology* **72**:53–96. DOI: https://doi.org/10.1016/bs.apha.2014.10.002, PMID: 25600367

Sigel E, Steinmann ME. 2012. Structure, function, and modulation of $_{GABA(A)}$ receptors. *The Journal of Biological Chemistry* **287**:40224–40231. DOI: https://doi.org/10.1074/jbc.R112.386664, PMID: 23038269

Smith SS, Shen H, Gong QH, Zhou X. 2007. Neurosteroid regulation of GABA(A) receptors: focus on the alpha4 and Delta subunits. *Pharmacology & Therapeutics* **116**:58–76. DOI: https://doi.org/10.1016/j.pharmthera.2007.03.008, PMID: 17512983

Steinbach JH, Akk G. 2001. Modulation of GABAA receptor channel gating by pentobarbital. *The Journal of Physiology* **537**:715–733. DOI: https://doi.org/10.1113/jphysiol.2001.012818

Stewart D, Desai R, Cheng Q, Liu A, Forman SA. 2008. Tryptophan mutations at azi-etomidate photo-incorporation sites on alpha1 or beta2 subunits enhance GABAA receptor gating and reduce etomidate modulation. *Molecular Pharmacology* **74**:1687–1695. DOI: https://doi.org/10.1124/mol.108.050500, PMID: 18805938

Sugasawa Y, Bracamontes JR, Krishnan K, Covey DF, Reichert DE, Akk G, Chen Q, Tang P, Evers AS, Cheng WWL. 2019. The molecular determinants of neurosteroid binding in the GABA(A) receptor. *The Journal of Steroid Biochemistry and Molecular Biology* **192**:105383. DOI: https://doi.org/10.1016/j.jsbmb.2019.105383, PMID: 31150831

Tong A, Petroff JT, Hsu FF, Schmidpeter PA, Nimigean CM, Sharp L, Brannigan G, Cheng WW. 2019. Direct binding of phosphatidylglycerol at specific sites modulates desensitization of a ligand-gated ion channel. *eLife* **8**:e50766. DOI: https://doi.org/10.7554/eLife.50766, PMID: 31724949

Trott O, Olson AJ. 2010. AutoDock vina: improving the speed and accuracy of docking with a new scoring function, efficient optimization, and multithreading. *Journal of Computational Chemistry* **31**:455–461. DOI: https://doi.org/10.1002/jcc.21334, PMID: 19499576

Ueno S, Zorumski C, Bracamontes J, Steinbach JH. 1996. Endogenous subunits can cause ambiguities in the pharmacology of exogenous gamma-aminobutyric acidA receptors expressed in human embryonic kidney 293 cells. *Molecular Pharmacology* **50**:931–938. PMID: 8863839

van Meer G, Voelker DR, Feigenson GW. 2008. Membrane lipids: where they are and how they behave. *Nature Reviews Molecular Cell Biology* **9**:112–124. DOI: https://doi.org/10.1038/nrm2330, PMID: 18216768

Vauquelin G, Van Liefde I, Swinney DC. 2015. Radioligand binding to intact cells as a tool for extended drug screening in a representative physiological context. *Drug Discovery Today: Technologies* **17**:28–34. DOI: https://doi.org/10.1016/j.ddtec.2015.09.001

Wang M, He Y, Eisenman LN, Fields C, Zeng CM, Mathews J, Benz A, Fu T, Zorumski E, Steinbach JH, Covey DF, Zorumski CF, Mennerick S. 2002. 3beta -hydroxypregnane steroids are pregnenolone sulfate-like GABA(A) receptor antagonists. *The Journal of Neuroscience* **22**:3366–3375. PMID: 11978813

Zhu S, Noviello CM, Teng J, Walsh RM, Kim JJ, Hibbs RE. 2018. Structure of a human synaptic $GABA_A$ receptor. *Nature* **559**:67–72. DOI: https://doi.org/10.1038/s41586-018-0255-3, PMID: 29950725

Zhu WJ, Vicini S. 1997. Neurosteroid prolongs GABAA channel deactivation by altering kinetics of desensitized states. *The Journal of Neuroscience* **17**:4022–4031. PMID: 9151718

Ziemba AM, Szabo A, Pierce DW, Haburcak M, Stern AT, Nourmahnad A, Halpin ES, Forman SA. 2018. Alphaxalone binds in inner transmembrane beta+-alpha- Interfaces of alpha1beta3gamma2 gamma-Aminobutyric acid type A receptors. *Anesthesiology* **128**:338–351. DOI: https://doi.org/10.1097/ALN.0000000000001978

Zorumski CF, Paul SM, Covey DF, Mennerick S. 2019. Neurosteroids as novel antidepressants and anxiolytics: gaba-a receptors and beyond. *Neurobiology of Stress* **11**:100196. DOI: https://doi.org/10.1016/j.ynstr.2019.100196, PMID: 31649968